

VARIATIONAL OPEN-DOMAIN QUESTION ANSWERING

Valentin Liévin^{1,2} **Andreas Geert Motzfeldt**¹ **Ida Riis Jensen**¹ **Ole Winther**^{1, 2, 3, 4}

¹ Section for Cognitive Systems, Technical University of Denmark, Denmark

² FindZebra, Denmark

³ Center for Genomic Medicine, Rigshospitalet, Copenhagen University Hospital, Denmark

⁴ Bioinformatics Centre, Department of Biology, University of Copenhagen, Denmark

{valv, olwi}@dtu.dk, andreas@motzfeldt.dk, ida.riis-jensen@hotmail.com

ABSTRACT

We introduce the Variational Open-Domain (VOD) framework for end-to-end training and evaluation of retrieval-augmented models (open-domain question answering and language modelling). We show that the Rényi variational bound, a lower bound to the task marginal likelihood, can be exploited to aid optimization and use importance sampling to estimate the task log-likelihood lower bound and its gradients using samples drawn from an auxiliary retriever (approximate posterior). The framework can be used to train modern retrieval-augmented systems end-to-end using tractable and consistent estimates of the Rényi variational bound and its gradients. We demonstrate the framework’s versatility by training reader-retriever BERT-based models on multiple-choice medical exam questions (MedMCQA and USMLE). We registered a new state-of-the-art for both datasets (MedMCQA: 62.9%, USMLE: 55.0%). Last, we show that the retriever part of the learned reader-retriever model trained on the medical board exam questions can be used in search engines for a medical knowledge base.

1 INTRODUCTION

The triad of the Transformer architecture Vaswani et al. (2017) coupled with massively parallel computing and trained with self-supervision on vast quantities of unlabelled text data has transformed the field of natural language processing. Instances of the Transformer architecture, such as BERT (Devlin et al., 2018) or GPT (Radford et al., 2018), have proven to be a valuable asset in several downstream problems such as question answering, named entity recognition, translation, and summarization.

There is a growing interest in scaling Transformer-based language models to using larger datasets and a gargantuan number of parameters. Scaling such models has resulted in sustained returns on many downstream tasks.¹ When applied to new tasks, large language models (LLMs) exploit the knowledge that was implicitly retained in their weights during training. However, implicit encoding of knowledge might be a factor that limits performances because i) the storage capacity of the model is bounded by the number of parameters, ii) controlling for the quality of the embedded knowledge is challenging iii) adapting to information that was not known at training time might require further pre-training.

Instead of relying solely on implicit knowledge, language models can be augmented with large external knowledge bases indexed with a retrieval mechanism. The technique was introduced initially as *open-domain question answering* (ODQA) to answer questions using the whole Wikipedia (Chen et al., 2017) and was later applied to language modelling (Guu et al., 2020; Lewis et al., 2020; Borgeaud et al., 2021; Izacard et al., 2022). Language models coupled with a retrieval mechanism might alleviate the shortcomings of implicit knowledge storage and retrieval because:

1. collections of documents can be arbitrarily large,

¹See a extensive benchmark of large language models in Srivastava et al. (2022) and collection of large language models in Brown et al. (2020); Rae et al. (2021); Chowdhery et al. (2022); Thoppilan et al. (2022); Hoffmann et al. (2022); Smith et al. (2022); Zhang et al. (2022); Lieber et al. (2021); Fedus et al. (2021); Laurençon et al. (2022)

2. knowledge is encoded as text and can therefore be more easily curated,
3. the knowledge base can be modified or replaced at inference time.

A wide range of tools is available to implement document retrieval, such as the time-proven BM25 (Chen et al., 2017), commercial search engines (Lazaridou et al., 2022) or deep retrievers built using language models. Unless there is a set of annotated evidence documents that are sufficiently aligned with the target task, as explored in Karpukhin et al. (2020); Qu et al. (2021); Khattab & Zaharia (2020), learning deep retriever is challenging. Lee et al. (2019) suggested modelling documents as a latent variable which support is the whole collection of documents. Nonetheless, optimizing latent variable models remains challenging, especially when modelling a discrete quantity.²

Contemporary research overcome training retrievers using a combination of (1) using annotated data Karpukhin et al. (2020); Qu et al. (2021); Khattab & Zaharia (2020), (2) learning from an auxiliary tasks such as the *inverse cloze task* (Lee et al., 2019; Izacard et al., 2021), and (3) estimating the marginal task likelihood and its gradient (Lee et al., 2019; Guu et al., 2020; Lewis et al., 2020; Sachan et al., 2021a; Paranjape et al., 2021), including disjoint training with *knowledge distillation* of the reader score into the retriever Yang & Seo (2020); Izacard & Grave (2020a).

We revisit retrieval-augmented modelling using Rényi divergence variational inference (Li & Turner, 2016). We introduce a probabilistic framework that allows estimating the marginal task likelihood and its gradients using samples drawn from an auxiliary retriever, or *approximate posterior*. The approximate posterior can be chosen as a checkpoint of the main retriever, designed to use the task target as input and/or trained jointly. We show that the Rényi variational bound, a lower bound of the task marginal lower bound, can be used for stable likelihood-based training. The framework is generic and can be applied to end-to-end joint optimization of extractive, generative and multiple-choice ODQA models as well as training of retrieval-augmented language models. We applied the framework to multiple-choice medical question-answering datasets. The main contributions of this paper are:

1. introducing the Variational Open-Domain (VOD), a probabilistic framework for end-to-end training, and evaluation of retrieval-augmented models,
2. introducing a truncated retriever parameterization that allows relaxing the standard top- K retriever approximation to using the top $P \geq K$,
3. deriving tractable estimates of a log-likelihood lower-bound and its gradients using documents sampled without replacement (priority sampling),
4. showing that our estimates are consistent (i.e. converge to their true expected value),
5. scoring a new state-of-the-art on the MedMCQA (62.9%) and USMLE (55.0%) datasets,
6. showing that a retriever learned using VOD is competitive with specialized search engines.

Furthermore, we release three datasets:

1. MedWiki: a subset of Wikipedia targeted to the MedMCQA and USMLE dataset,
2. FindZebra corpus: a collection of 30.7k articles about rare diseases,
3. FindZebra queries: a subset of real-user search queries related to rare disease diagnosis.

2 A PROBABILISTIC FRAMEWORK FOR RETRIEVAL-AUGMENTED TASKS

In this section, we introduce Variational Open-Domain (VOD) framework in three acts. We introduce the Rényi variational bound and its gradients. We describe a top- P truncated retriever parameterization with $P \leq N$ where N is the number of documents in the corpus. We detail a method for tractable estimation of the bound and its gradients using importance sampling with $K \leq P \leq N$ samples.

²Learn more about discrete latent variable optimization in Hinton et al. (1995); Le et al. (2018); Mnih & Gregor (2014); Mnih & Rezende (2016); van den Oord et al. (2017); Tucker et al. (2017); Grathwohl et al. (2017); Masrani et al. (2019); Liévin et al. (2020).

2.1 LOG-LIKELIHOOD LOWER BOUND AND GRADIENT

Let a question \mathbf{q} be defined in a space Ω (e.g., the space of sequences of tokens) and the set of possible answers be $\mathbb{A} \subset \Omega$ with a correct answer denoted $\mathbf{a} \in \mathbb{A}$. We introduce a corpus of N documents $\mathbb{D} := \{\mathbf{d}_1, \dots, \mathbf{d}_N\} \in \Omega^N$. In open-domain tasks, we are interested in modelling the marginal task likelihood using a joint model $p_\theta(\mathbf{a}, \mathbf{d} \mid \mathbf{q})$ parameterized by θ :

$$p_\theta(\mathbf{a} \mid \mathbf{q}) := \sum_{\mathbf{d} \in \mathbb{D}} p_\theta(\mathbf{a}, \mathbf{d} \mid \mathbf{q}). \quad (1)$$

RÉNYI DIVERGENCE VARIATIONAL INFERENCE

We adopt a reader-retriever factorization of the joint-model $p_\theta(\mathbf{a}, \mathbf{d} \mid \mathbf{q}) := p_\theta(\mathbf{a} \mid \mathbf{d}, \mathbf{q})p_\theta(\mathbf{d} \mid \mathbf{q})$ and apply Rényi divergence variational inference (Li & Turner, 2016) to estimate the marginal task likelihood using samples from an approximate posterior $r_\phi(\mathbf{d} \mid \mathbf{a}, \mathbf{q})$. The approximate posterior, with parameters ϕ , can be defined using either a keyword-search engine (BM25), a checkpoint of $p_\theta(\mathbf{d} \mid \mathbf{q})$, or another model learned jointly. Given a parameter $\alpha < 1$, and the importance weight $w_{\theta, \phi}(\mathbf{a}, \mathbf{d}) := p_\theta(\mathbf{a}, \mathbf{d} \mid \mathbf{q}) / r_\phi(\mathbf{d} \mid \mathbf{a}, \mathbf{q})$, we introduce the variational Rényi bound (RVB):

$$\mathcal{L}_\alpha(\mathbf{a}, \mathbf{q}) := \frac{1}{1 - \alpha} \log \mathbb{E}_{r_\phi(\mathbf{d} \mid \mathbf{a}, \mathbf{q})} \left[w_{\theta, \phi}^{1 - \alpha}(\mathbf{a}, \mathbf{d}, \mathbf{q}) \right]. \quad (2)$$

The RVB is a lower bound of the marginal log-likelihood for $\alpha \geq 0$ its definition is extended in $\alpha = 1$ by continuity using $\mathcal{L}_{\alpha=1}(\mathbf{a}, \mathbf{q}) := \lim_{\alpha \rightarrow 1} \mathcal{L}_\alpha(\mathbf{a}, \mathbf{q})$, which corresponds to the variational lower-bound (ELBO Jordan et al. (1999)) denoted $\mathcal{L}_{\text{VI}}(\mathbf{a}, \mathbf{d})$. The three main properties of the RVB are:

$$\mathcal{L}_{\alpha=0}(\mathbf{a}, \mathbf{q}) = \log p_\theta(\mathbf{a} \mid \mathbf{q}) \quad (3)$$

$$\mathcal{L}_{\alpha \geq 0}(\mathbf{a}, \mathbf{q}) \leq \log p_\theta(\mathbf{a} \mid \mathbf{q}) \quad (4)$$

$$\mathcal{L}_{\alpha=1}(\mathbf{a}, \mathbf{q}) = \mathbb{E}_{r_\phi(\mathbf{d} \mid \mathbf{a}, \mathbf{q})} [\log p_\theta(\mathbf{a} \mid \mathbf{d}, \mathbf{q})] - D_{\text{KL}} [r_\phi(\mathbf{d} \mid \mathbf{a}, \mathbf{q}) \parallel p_\theta(\mathbf{d} \mid \mathbf{q})] := \mathcal{L}_{\text{VI}}(\mathbf{a}, \mathbf{q}). \quad (5)$$

GRADIENTS

The gradient of RVB w.r.t. the parameter θ are

$$\nabla_\theta \mathcal{L}_\alpha(\mathbf{a}, \mathbf{q}) = \mathbb{E}_{r_\phi(\mathbf{d} \mid \mathbf{a}, \mathbf{q})} \left[\widetilde{w}_{\theta, \phi}^{1 - \alpha}(\mathbf{a}, \mathbf{d}, \mathbf{q}) \nabla_\theta \log p_\theta(\mathbf{a}, \mathbf{d} \mid \mathbf{q}) \right] \quad (6)$$

where the normalized weights are defined as $\widetilde{w}_{\theta, \phi}^{1 - \alpha}(\mathbf{a}, \mathbf{d}) := \frac{w_{\theta, \phi}^{1 - \alpha}(\mathbf{a}, \mathbf{d}, \mathbf{q})}{\mathbb{E}_{r_\phi(\mathbf{d}' \mid \mathbf{a}, \mathbf{q})} [w_{\theta, \phi}^{1 - \alpha}(\mathbf{a}, \mathbf{d}', \mathbf{q})]}$.

In this paper, we consider the approximate posterior r_ϕ to be static and therefore do not estimate the gradient w.r.t. the approximate posterior. Optimizing the parameter ϕ jointly with θ can be done by application of importance sampling coupled with variance reduction techniques (Burda et al., 2015; Mnih & Rezende, 2016; Le et al., 2018; Masrani et al., 2019; Kool et al., 2019b; Liévin et al., 2020).

STABILIZING TRAINING USING THE RVB

For $\alpha = 0$, the exact gradient of the parameter θ allows maximizing the marginal task likelihood, which in expectation is independent of the choice of the approximate posterior. However, during early training, the joint model $p_\theta(\mathbf{a}, \mathbf{d} \mid \mathbf{q})$ might be uninformative and so might be the weight $w_{\theta, \phi}(\mathbf{a}, \mathbf{d}, \mathbf{q})$ and the exact gradient in equation 6.

Optimizing the joint model $p_\theta(\mathbf{a}, \mathbf{d} \mid \mathbf{q})$ using the ELBO coupled with an informative approximate posterior circumvents this problem. For $\alpha = 1$, the RVB matches the ELBO and the gradients restricted to the reader and retriever parameters are

$$\nabla_{\theta(\text{READER})} \mathcal{L}_{\alpha=1}(\mathbf{a}, \mathbf{q}) = \mathbb{E}_{r_\phi(\mathbf{d} \mid \mathbf{a}, \mathbf{q})} [\nabla_\theta \log p_\theta(\mathbf{a} \mid \mathbf{d}, \mathbf{q})] \quad (7)$$

$$\nabla_{\theta(\text{RETRIEVER})} \mathcal{L}_{\alpha=1}(\mathbf{a}, \mathbf{q}) = -\nabla_\theta D_{\text{KL}} [r_\phi(\mathbf{d} \mid \mathbf{a}, \mathbf{q}) \parallel p_\theta(\mathbf{d} \mid \mathbf{q})]. \quad (8)$$

Maximizing the ELBO corresponds to optimizing the reader and the retriever disjointly. On the reader side, this equals maximizing the answer likelihood $p_\theta(\mathbf{a} \mid \mathbf{d}, \mathbf{q})$ in expectation over $r_\phi(\mathbf{d} \mid \mathbf{a}, \mathbf{q})$ independently of the value of $p_\theta(\mathbf{d} \mid \mathbf{q})$. On the retriever side, this corresponds to matching the approximate posterior with the learned retriever $p_\theta(\mathbf{d} \mid \mathbf{q})$. This can be seen as an instance of knowledge distillation of the posterior into the retriever. After an initial learning phase, the RVB can be smoothly interpolated from the ELBO to the marginal task likelihood by controlling the parameter α .

2.2 TRACTABLE ESTIMATION OF THE RVB

Computational efficiency is a key challenge in retrieval-augmented modelling. Under a budget of K documents per question, we introduce a general definition of the retrievers that allows for relaxing the top- K approximation of the retriever to using the top $P \geq K$ documents. Using sampling without replacement, we then define a tractable and consistent estimate of the RVB and its gradient.

TRUNCATED RETRIEVER PARAMETERIZATION

Algorithm 1 Two-step sampling using truncated retrievers using efficient top- P retrieval.

Require: $\mathbf{q}, \mathbb{D} = \{\mathbf{d}_1, \dots, \mathbf{d}_N\} \in \Omega^N, K \leq P \leq N, f_\phi : \Omega^2 \rightarrow \mathbb{R}$

- 1: $\mathbb{T}_\phi \leftarrow \text{argtop}_{\mathbf{d} \in \mathbb{D}}(f_\phi(\mathbf{d}, \mathbf{q}); P)$ // retrieve P documents using MIPS or BM25
- 2: $\mathbf{d} \sim r_\phi(\mathbf{d} \mid \mathbf{q}) \propto \mathbb{1}[\mathbf{d} \in \mathbb{T}_\phi] \exp f_\phi(\mathbf{d}, \mathbf{q})$ // sample \mathbf{d} from the truncated multinomial

The distributions $p_\theta(\mathbf{d} \mid \mathbf{q})$ and $r_\phi(\mathbf{d} \mid \mathbf{a}, \mathbf{q})$ are defined on a potentially large number of documents and, therefore, must be chosen with care to ensure the scalable estimation of the RVB. We parameterize the retrieval distributions using score functions $f_\theta : \Omega^2 \rightarrow \mathbb{R}$ and $f_\phi : \Omega^3 \rightarrow \mathbb{R}$ and restrict the both distributions to the set \mathbb{T}_ϕ defined as the top $P \leq N$ documents ranked by the score $f_\phi(\mathbf{a}, \mathbf{d}, \mathbf{q})$:

$$p_\theta(\mathbf{d} \mid \mathbf{q}) := \frac{\mathbb{1}[\mathbf{d} \in \mathbb{T}_\phi] \exp f_\theta(\mathbf{d}, \mathbf{q})}{\sum_{\mathbf{d}' \in \mathbb{T}_\phi} \exp f_\theta(\mathbf{d}', \mathbf{q})}, \quad r_\phi(\mathbf{d} \mid \mathbf{a}, \mathbf{q}) := \frac{\mathbb{1}[\mathbf{d} \in \mathbb{T}_\phi] \exp f_\phi(\mathbf{a}, \mathbf{d}, \mathbf{q})}{\sum_{\mathbf{d}' \in \mathbb{T}_\phi} \exp f_\phi(\mathbf{a}, \mathbf{d}, \mathbf{q}')} . \quad (9)$$

The score function f_θ and f_ϕ can be implemented using BM25 and/or contextual vector representations extracted using pretrained language models such as DPR or ColBERT. For instance using a dual-encoder model $f_\theta(\mathbf{d}, \mathbf{q}) = \text{BERT}_\theta(\mathbf{d})^T \text{BERT}_\theta(\mathbf{q})$ and $f_\phi(\mathbf{a}, \mathbf{d}, \mathbf{q}) = \text{BERT}_\phi([\mathbf{q}; \mathbf{a}])^T \text{BERT}_\phi(\mathbf{d})$ where BERT is the function that return the output of a BERT model at the CLS token and $[\cdot; \cdot]$ is the concatenation operator. Sampling documents using the truncated distribution can be split into a two-step process described in Algorithm 1. The process can be efficiently implemented using `elasticsearch`³ and/or `faiss` (Johnson et al., 2021).

The framework allows using full-range retrievers with $P = N$. However, using the truncated retrievers with $P \ll N$ comes with two advantages: i) only the top- P document scores need to be cached or retained in memory, and ii) the value P controls an exploration-exploitation threshold: a higher value of P allows sampling a greater diversity of documents (*exploration*), but a smaller value makes it more likely that all documents in the set \mathbb{T}_ϕ will be visited during training (*exploitation*).

IMPORTANCE SAMPLING ESTIMATES

Priority sampling We define $\mathbb{S} = \{\mathbf{d}_1, \dots, \mathbf{d}_K\} \subset \mathbb{T}_\phi$ a set of documents sampled without replacement from $r_\phi(\mathbf{d} \mid \mathbf{a}, \mathbf{q})$ using *priority sampling* (Duffield et al., 2007). The sampling procedure comes with importance weights $s(\mathbf{d}_1), \dots, s(\mathbf{d}_K)$ defined such that for a function $h(\mathbf{d})$, $\sum_{\mathbf{d} \in \mathbb{S}} s(\mathbf{d}) h(\mathbf{d}) \approx \mathbb{E}_{r_\phi(\mathbf{d} \mid \mathbf{a}, \mathbf{q})} [h(\mathbf{d})]$. Standard priority sampling is unbiased but might suffer from large variance. Therefore, we use a lower-variance self-normalized estimate (Kool et al., 2019a) with weights $\bar{s}(\mathbf{d}) = s(\mathbf{d}) / \sum_{\mathbf{d}' \in \mathbb{S}} s(\mathbf{d}')$. Self-normalized priority sampling 1) guarantees optimal allocation of the computing resources by avoiding sampling the same documents multiple times, 2) yields estimates that are, in general, of a lower variance than those estimated using Monte-Carlo with replacement, and 3) is unbiased in the limit $K = P$. We detail priority sampling in Appendix A.

³<http://www.elastic.co/>

RVB estimation In Appendix B, we derived importance-weighted estimates of the RVB and included a discussion about their properties. In this section, we present the results of our derivations.

Evaluating the normalizing constant of $p_\theta(\mathbf{d} \mid \mathbf{q})$ at every training iteration is prohibitively expensive (complexity $\mathcal{O}(P)$). Instead, we utilize the un-normalized retrieval density ratio $\zeta(\mathbf{d}) := \exp f_\theta(\mathbf{d}, \mathbf{q}) / \exp f_\phi(\mathbf{a}, \mathbf{d}, \mathbf{q})$ and estimate the RVB with:

$$\mathcal{L}_\alpha(\mathbf{a}, \mathbf{q}) \approx \hat{\mathcal{L}}_\alpha^S(\mathbf{a}, \mathbf{q}) := \frac{1}{1-\alpha} \log \sum_{\mathbf{d} \in S} \tilde{s}(\mathbf{d}) \left(\frac{p_\theta(\mathbf{a} \mid \mathbf{d}, \mathbf{q}) \zeta(\mathbf{d})}{\sum_{\mathbf{d}' \in S} \tilde{s}(\mathbf{d}') \zeta(\mathbf{d}')} \right)^{1-\alpha} \quad (10)$$

$$\text{and the gradient with } \nabla_\theta \mathcal{L}_\alpha(\mathbf{a}, \mathbf{q}) \approx \sum_{\mathbf{d} \in S} \tilde{s}(\mathbf{d}) \widetilde{w}_{\theta, \phi}^{1-\alpha}(\mathbf{a}, \mathbf{d} \mid S) \nabla_\theta \log p_\theta(\mathbf{a}, \mathbf{d} \mid \mathbf{q}) \quad (11)$$

$$\text{where } \widetilde{w}_{\theta, \phi}^{1-\alpha}(\mathbf{a}, \mathbf{d} \mid S) := \frac{(\zeta(\mathbf{d}) p_\theta(\mathbf{a} \mid \mathbf{d}, \mathbf{q}))^{1-\alpha}}{\sum_{\mathbf{d}' \in S} \tilde{s}(\mathbf{d}') (\zeta(\mathbf{d}') p_\theta(\mathbf{a} \mid \mathbf{d}', \mathbf{q}))^{1-\alpha}}. \quad (12)$$

The term $\nabla_\theta \log p_\theta(\mathbf{a}, \mathbf{d} \mid \mathbf{q}) = \nabla_\theta \log p_\theta(\mathbf{a} \mid \mathbf{d}, \mathbf{q}) + \nabla_\theta \log p_\theta(\mathbf{d} \mid \mathbf{q})$ also requires an approximation to avoid expensive evaluations of the normalizing constant of $p_\theta(\mathbf{d} \mid \mathbf{q})$:

$$\nabla_\theta \log p_\theta(\mathbf{d} \mid \mathbf{q}) \approx \nabla_\theta f_\theta(\mathbf{d}, \mathbf{q}) - \sum_{\mathbf{d}' \in S} \frac{\tilde{s}(\mathbf{d}') \zeta(\mathbf{d}')}{\sum_{\mathbf{d}'' \in S} \tilde{s}(\mathbf{d}'') \zeta(\mathbf{d}'')} \nabla_\theta f_\theta(\mathbf{d}', \mathbf{q}). \quad (13)$$

All above estimates are of complexity $\mathcal{O}(K)$ and are consistent (i.e., converge to the true expected value in the limit $K = P$ with probability one). Furthermore, the standard importance-weighted bound that we estimate with $\hat{\mathcal{L}}_{\alpha=0}^S(\mathbf{a}, \mathbf{q})$ is guaranteed to approximate the marginal task log-likelihood more tightly as $K \rightarrow P$ (Burda et al., 2015).

3 APPLICATION TO MULTIPLE-CHOICE ODQA

In this section, we detail how to apply the VOD framework to multiple-choice question answering. Nonetheless, VOD is general-purpose and we also detail how to apply VOD to generative and extractive ODQA as well as to retrieval-augmented language modelling and FiD in Appendix C.

In the multiple-choice setting, we consider a vector of M answer options $\mathbf{A} := [\mathbf{a}_1, \dots, \mathbf{a}_M]$ and denote \star the index of the correct option. We define the vector of M queries as $\mathbf{Q} = [\mathbf{q}_1, \dots, \mathbf{q}_M]$ with $\mathbf{q}_j := [\mathbf{q}; \mathbf{a}_j]$ corresponding to the question concatenated with the answer option of index j . We denote a vector of M documents $\mathbf{D} = [\mathbf{d}_1, \dots, \mathbf{d}_M] \in \mathbb{D}^M$ and the set of M combinations of documents as $\mathbb{D}^{(M)}$, which contains N^M document vectors. We model the marginal likelihood as

$$p_\theta(\mathbf{a}_\star \mid \mathbf{Q}) := \sum_{\mathbf{D} \in \mathbb{D}^{(M)}} p_\theta(\mathbf{D} \mid \mathbf{Q}) p_\theta(\mathbf{a}_\star \mid \mathbf{D}, \mathbf{Q}) \quad (14)$$

and introduce another score function denoted $g_\theta : \Omega^2 \rightarrow \mathbb{R}$ to parameterize the reader. We adopt a per-option truncated retriever $p_\theta(\mathbf{d} \mid \mathbf{q})$ parameterized by a score f_θ as described in equation 9. The reader and retriever models are defined as

$$p_\theta(\mathbf{a}_\star \mid \mathbf{D}, \mathbf{Q}) := \frac{\exp g_\theta(\mathbf{d}_\star, \mathbf{q}_\star)}{\sum_{j=1}^M \exp g_\theta(\mathbf{d}_j, \mathbf{q}_j)}, \quad p_\theta(\mathbf{D} \mid \mathbf{Q}) := \prod_{j=1}^M p_\theta(\mathbf{d}_j \mid \mathbf{q}_j). \quad (15)$$

The approximate posterior is modelled as $r_\phi(\mathbf{D} \mid \mathbf{A}, \mathbf{Q}) = r_\phi(\mathbf{D} \mid \mathbf{Q}) = \prod_{j=1}^M r_\phi(\mathbf{d}_j \mid \mathbf{q}_j)$ where $r_\phi(\mathbf{d}_j \mid \mathbf{q}_j) = r_\phi(\mathbf{d}_j \mid \mathbf{a}_j, \mathbf{q})$. $r_\phi(\mathbf{d}_j \mid \mathbf{q}_j)$ adopts the truncated parameterization described in equation 9 with score function $f_\phi(\mathbf{d}, \mathbf{q})$. The RVB can be applied to $p_\theta(\mathbf{a}_\star \mid \mathbf{Q})$ and so can the bound and gradient estimates derived in sections 10 and 11. Estimating the RVB in the multiple-choice setting requires sampling K documents per answer option. Read more details in Appendix C.3.

4 RELATED WORK

The VOD framework can be applied to evaluate and train model targeted to various tasks such as question answering and language modelling (see Appendix C). Therefore, rather than focusing on the

Table 1: Overview of retriever training techniques for a selection of retrieval-augmented methods. We report whether the retriever is learned end-to-end with the reader (e.g., maximum likelihood), whether the document retrieval mechanism can be conditioned on the task target (e.g., answer), and report the range of the documents accessible at each training step (retriever support).

Method	Retriever training	End-to-end retriever learning	Target-aware retrieval	Retriever support
DPR (Karpukhin et al., 2020)	Supervised	✗	✓	top- K doc.
ColBERT (Khattab et al., 2021)	Supervised	✗	✓	top- K doc.
Contriever (Izacard et al., 2021)	Self-supervised (improved ICT)	✗	—	—
FiD (Izacard & Grave, 2020b)	Frozen DPR dual-encoder	✗	✗	top- K doc
RETRO (Borgeaud et al., 2021)	Frozen BERT dual-encoder	✗	✗	top- K doc
ORQA (Lee et al., 2019)	ICT + Marginal LL* + frozen BERT doc. encoder	(✓)	✗	top- K doc.
RAG (Lewis et al., 2020)	Marginal LL* + frozen DPR doc. encoder	(✓)	✗	top- K doc.
REALM (Guu et al., 2020)	ICT + Marginal LL*	✓	✗	top- K doc.
EMDR ² Sachan et al. (2021b)	ICT + Expectation-Maximization	✓	✗	top- K doc.
Hindsight (Paranjape et al., 2021)	ColBERT init. + ELBO + marginal LL*	✓	✓	top- K doc.
VOD	Rényi variational bound	✓	✓	top- P doc. [†]

*LL: likelihood, [†] $K \leq P \leq N$ (K the number of documents that fit in a training batch, N is the size of the corpus, P is chosen)

implementation, we discuss alternatives to optimizing deep retrievers. We present an overview of the related methods with their corresponding references in Table 1.

Supervised retriever learning ORQA introduced the *inverse cloze task* (ICT), a self-supervised task consisting in learning to match a text passage with its context. The ICT enables zero-shot retrieval and has been widely adopted as a pretraining scheme. In contrast to this self-supervised approach, DPR leverages questions paired with human-annotated and/or weakly-classified documents. DPR remains a popular solution and is now found in various retrieval-augmented systems such as RAG and FiD.

Top- K marginal likelihood ORQA, REALM, RAG all consider differentiating the top- K approximated marginal likelihood $p_\theta(\mathbf{a} \mid \mathbf{q}) = \sum_{\mathbf{d} \in \mathbb{T}_\phi} p_\theta(\mathbf{a}, \mathbf{d} \mid \mathbf{q})$ where \mathbb{T}_ϕ is the batch of top $K = P$ documents. EMDR² and Hindsight also optimize the top- K marginal likelihood by maximizing proxy objectives. EMDR² relies on an Expectation-Maximization objective evaluated under the posterior $p_\theta(\mathbf{d} \mid \mathbf{a}, \mathbf{q}) \propto p_\theta(\mathbf{d} \mid \mathbf{q})p_\theta(\mathbf{a} \mid \mathbf{d}, \mathbf{q})$. Hindsight optimizes the variational lower-bound (ELBO) (Jordan et al., 1999) evaluated under a label-aware approximate posterior $r_\phi(\mathbf{d} \mid \mathbf{a}, \mathbf{q})$.

Variational Inference Maximizing the ELBO is effective as long as the inference gap $D_{\text{KL}}(r_\phi(\mathbf{d} \mid \mathbf{a}, \mathbf{q}) \parallel p_\theta(\mathbf{d} \mid \mathbf{a}, \mathbf{q})) = \log p_\theta(\mathbf{a}) - \mathcal{L}_{\text{VI}}(\mathbf{a}, \mathbf{d})$ remains sufficiently small (see Cremer et al. (2018)). Too large of a gap results in a discrepancy between training under $r_\phi(\mathbf{d} \mid \mathbf{a}, \mathbf{q})$ and evaluating under $p_\theta(\mathbf{d} \mid \mathbf{q})$. Hindsight solves this issue by progressively replacing samples from $r_\phi(\mathbf{d} \mid \mathbf{a}, \mathbf{q})$ with samples from $p_\theta(\mathbf{d} \mid \mathbf{q})$ during training. Using only samples from $p_\theta(\mathbf{d} \mid \mathbf{q})$ corresponds to using the top- K marginal likelihood. VOD utilizes a tight log-likelihood lower bound (Burda et al., 2015) that we approximate with $\hat{L}_{\alpha=0}^{\mathbb{S}_\phi}$. In VOD, the tight lower bound can be interpolated with a looser bound, the ELBO, by adjusting the parameter α . In contrast to Hindsight, our approach does not require altering the sampling process. Aiding optimization with interpolating the RVB bound has been explored in Liévin et al. (2020).

Indexing, caching and sampling Re-indexing the corpus at every step is prohibitively expensive. Therefore, evaluating the marginal likelihood using samples from the trained retriever is too costly. ORQA, RAG, and RETRO overcome this issue by freezing part of the retriever. REALM, EMDR², and Hindsight evaluate the objective asynchronously or periodically cached retriever scores, which results in unaccounted approximations. VOD allows caching the retriever scores while keeping the retriever fully trainable, thanks to modelling the retrieval process explicitly. Last, VOD introduces a truncated retriever parameterization that generalizes the top- K common retrieval approximation and allows handling a retriever using the entire corpus as support. However, we found that, in practice, it is beneficial to restrict retrieval to the top- P documents with $P \geq K$ (exploration/exploitation trade-off).

Table 2: Summary of the medical question answering datasets and the information retrieval benchmark. The number of tokens is measured for the base BioLinkBERT tokenizer, the *mean [min. – max.]* values are reported.

	MedMCQA	USMLE	FZ Queries
Answer type	multiple-choice	multiple-choice	CUI (UMLS)
# questions (train/valid./test)	182.8k / 4.2k / 6.1k	10.2k / 1.3k / 1.3k	– / – / 248
# tokens per question	19 [4 – 349]	158 [13 – 801]	17 [8 – 89]
# tokens per answer option	5 [3 – 60]	6.6 [3 – 61]	–
Source	AIIMS and NEET PG entrance exams	National Medical Board Examination (US)	search queries registered on FindZebra

5 EXPERIMENTS

We present the tasks and datasets in the medical domain, showcase results on end-to-end multiple-choice ODQA, and apply the trained models to information retrieval. The code for all experiments is available at <http://github.com/vlievin/fz-openqa>.

5.1 DATA

The medical multiple-choice question answering datasets and the corpora are summarized in Table 2.

MedMCQA Pal et al. (2022) is a large-scale multiple-choice question answering collected from Indian medical school entrance exams (AI-IMS and NEET-PG). The MedMCQA covers a broad range of medical topics (dentistry, pathology, surgery, preventive medicine, etc.) and many question types (diagnosis, recalling expert factual knowledge, mathematical problem, etc.)

MedWiki We introduce the MedWiki corpus, a collection of 4.5% of articles taken from the English Wikipedia and targeted to the MedMCQA and USMLE datasets. The MedWiki corpus was built by querying each answer option from the MedMCQA and USMLE datasets against the Wikipedia API. Read more in Appendix G.

USMLE Jin et al. (2021) is a collection of medical questions gathered from the US medical board exam. The questions aim to assess human doctors’ medical knowledge and demonstrate decision-making. Each question includes a medical history followed by the vital signs (e.g., blood pressure, temperature), and possibly a specific analysis (e.g., CT-scan).

	MedWiki	FindZebra
# articles	293.6k	30.7k
# passages	7,766.9k	711.9k

Table 3: Summary of the medical corpora.

FindZebra corpus & queries FindZebra is a search tool for helping the diagnosis of rare diseases. It is built on open source information retrieval software (BM25) tailored to the problem.⁴ The FindZebra corpus indexes a collection of curated articles gathered from GARD, GeneReviews, Genetics Home Reference, OMIM, Orphanet, and Wikipedia. Each article is referenced with a Concept Unique Identifier (CUI)⁵. Additionally, we release a collection of 280 search queries (FZ queries) recorded on the platform. Each query is annotated with a CUI corresponding to the reference search result.

The FindZebra and MedWiki datasets are available at <http://huggingface.co/findzebra>.

5.2 ODQA EXPERIMENTAL SETUP

We implement the retriever using a DPR-like dual-encoder with a shared backbone and implement the multiple-choice reader following Devlin et al. (2018). We use the domain-specific BioLinkBERT Yasunaga et al. (2022) as the backbone for both models and the MedWiki corpus for all QA experiments.

⁴<http://findzebra.com>

⁵CUIs are part of the Unified Medical Language System (UMLS, Bodenreider (2004))

All experiments run on a single machine with eight RTX 5000 GPUs using half-precision for training and evaluation. We provide further details in Appendix E.

Hybrid approximate posterior We parameterize the score f_ϕ of the posterior using a composite BM25 score combined with a checkpoint of the retriever score f_θ denoted f_ϕ^{ckpt} . Specifically, we use

$$f_\phi(\mathbf{a}, \mathbf{d}, \mathbf{q}) := f_\phi^{\text{ckpt}}(\mathbf{d}, [\mathbf{q}; \mathbf{a}]) + \tau^{-1} (\text{BM25}(\mathbf{q}, \mathbf{d}) + \beta \cdot \text{BM25}(\mathbf{a}, \mathbf{d})) . \quad (16)$$

where $\tau = 5$ and β is a parameter scaled proportionally to the ratio of question and answer lengths L_q/L_a to ensure that the BM25 score of the question does not outweigh the answer score. We use $\beta = 1 + 0.5 \max \{0, \log (L_q/L_a)\}$. At initialization f_θ is uninformative and thus we set $f_\phi^{\text{ckpt}} = 0$

Training, indexing and annealing We organize the training into rounds of T steps as in Khattab et al. (2021). At the beginning of each period, for each question-answer pair \mathbf{q}_j , we retrieve the set of top- P documents \mathbb{T}_ϕ and cache the set of values $\{f_\phi(\mathbf{d}, \mathbf{q}, \mathbf{a}_j) \mid \mathbf{d} \in \mathbb{T}_\phi\}$, except for the first period where f_ϕ^{ckpt} is set to zero. During the first training round, we anneal the RVB parameter α from 1 to 0 to stabilize early training by distilling the BM25 cached score $f_\phi(\mathbf{a}, \mathbf{d}, \mathbf{q}) = 0 + \tau^{-1} (\text{BM25}(\mathbf{q}, \mathbf{d}) + \beta \cdot \text{BM25}(\mathbf{a}, \mathbf{d}))$ into the trainable retriever score $f_\theta(\mathbf{d}, \mathbf{q})$, as pictured in Figure 1. At each training iteration, we sample a set of $K = 8$ document \mathbb{T}_ϕ for each of the $M = 4$ question-answer pairs and estimate the RVB and its gradient using the cached values $f_\phi(\mathbf{d}, \mathbf{q}, \mathbf{a}_j)$.

Data augmentation The USMLE dataset is small and thus prone to overfitting. We tested training with a concatenated dataset and training first on the MedMCQA, and then on the USMLE.

Baselines We compare the VOD framework with models reported in the literature and with the human baseline. All models reported in the literature are trained disjointly, corresponding to a setup identical to DrQA Chen et al. (2017). We trained disjoint BioLinkBERT readers with a BM25 retrievers by applying VOD with $f_\theta(\mathbf{a}, \mathbf{d}, \mathbf{q}) = f_\phi(\mathbf{a}, \mathbf{d}, \mathbf{q}) = \text{BM25}(\mathbf{q}, \mathbf{d}) + \beta \cdot \text{BM25}(\mathbf{a}, \mathbf{d})$. We report the current state-of-the-art obtained using zero-shot GPT-3 combined with a BM25 retriever and Chain-of-Thought (CoT) prompting Kojima et al. (2022). All the MedMCQA baselines use Wikipedia as a knowledge base, whereas the USMLE baselines use the original MedQA corpus of 18 medical textbooks. We use the MedWiki corpus in all experiments.

Evaluation We estimate the likelihood for each answer option using $C = 10$ Monte-Carlo samples, each containing $MK = 4 \cdot 8 = 32$ documents using the estimates defined in equation 49.

5.3 ODQA ACCURACY

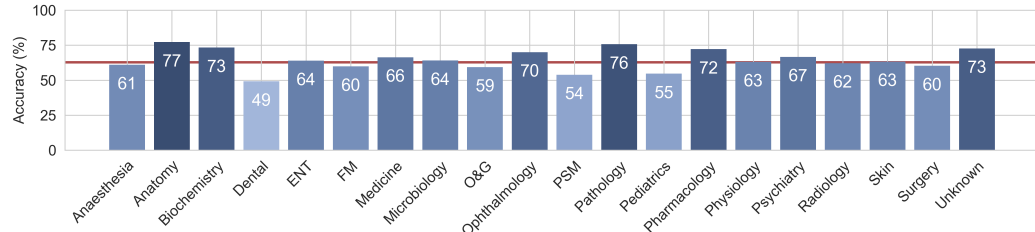


Figure 2: Per-category MedMCQA test accuracy for the VOD model trained on MedMCQA.

Table 4: Open-domain question answering accuracy on the MedMCQA dataset.

Method	Reader	Retriever	QA training set	Valid.	Test
VOD	BioLinkBERT	BM25	MedMCQA	51.6	55.3
VOD	BioLinkBERT	BioLinkBERT	MedMCQA	58.3	62.9
Uniform baseline	–	–	–	25.0	25.0
Disjoint ¹	PubMedBERT	DPR	MedMCQA	43.0	47.0
Zero-shot prompting ²	GPT-3	–	–	44.0	–
Zero-shot prompting ²	GPT-3	BM25	–	46.7	–
Zero-shot CoT prompting ²	GPT-3	BM25	–	48.8	–
Human (passing score) ²	–	–	–	≥ 50	≥ 50
Human (merit candidate) ²	–	–	–	≥ 90	≥ 90

¹Pal et al. (2022), ²Liévin et al. (2022)

MedMCQA We report the validation and test accuracy of the VOD framework applied to BioLinkBERT (base) and the baselines in Table 4. VOD outperforms both the disjoint BERT-based and the GPT-3 based with a new state-of-the-art test accuracy of 62.9%, an improvement of +15.9% over the disjoint PubMedBERT reader coupled with a DPR retriever, and +7.6% improvement over the BioLinkBERT reader with static BM25 retriever. Compared to the zero-shot GPT-3 coupled with a simple BM25 retriever, VOD is 9.5% more accurate on the validation set.

In figure 2, we report the accuracy of the VOD model trained on MedMCQA for each of the question categories reported in the test set. VOD performed exceptionally well (>70% test accuracy) for the question related to anatomy, biochemistry, pathology, and pharmacology but performed significantly worse (<60%) in dentistry, paediatrics, obstetrics and gynaecology (O&G), and Preventive & Social Medicine (PSM).

Table 5: Open-domain question answering accuracy on the USMLE dataset.

Method	Reader	Retriever	QA training set	Valid.	Test
VOD	BioLinkBERT	BM25	USMLE	41.0	40.4
VOD	BioLinkBERT	BioLinkBERT	USMLE	45.8	44.7
VOD	BioLinkBERT	BioLinkBERT	MedMCQA	47.2	46.8
VOD	BioLinkBERT	BioLinkBERT	MedMCQA → USMLE	53.6	55.0
Uniform baseline	–	–	–	25.0	25.0
Custom BM25 ¹	–	BM25	–	38.3	36.1
Disjoint ²	PubMedBERT	BM25	USMLE	–	38.1
Disjoint ³	BioLinkBERT	BM25	USMLE	–	40.0
Disjoint ³	BioLinkBERT-L	BM25	USMLE	–	44.6
Zero-shot prompting ⁴	GPT-3	–	–	–	46.0
Zero-shot prompting ⁴	GPT-3	BM25	–	–	47.3
Zero-shot CoT prompting ⁴	GPT-3	BM25	–	–	53.1
Human (passing score) ⁴	–	–	–	≥ 60	≥ 60

¹Jin et al. (2021), ²Gu et al. (2021), ³Yasunaga et al. (2022), ⁴Liévin et al. (2022)

USMLE We report the validation and test accuracy in Table 5. We found that using VOD with a BioLinkBERT backbone outperforms a BioLinkBERT reader coupled with a BM25 retriever, even when using the larger version of BioLinkBERT (44.7% for VOD, 40.0% for disjoint BioLinkBERT, 44.6% for the disjoint large BioLinkBERT).

We found that pretraining ODQA models on the large MedMCQA results in higher accuracy on the USMLE dataset. A VOD model pretrained on the MedMCQA delivers 46.8% test accuracy in a zero-shot setting and a state-of-the-art of 55.0% test accuracy with further USMLE fine-tuning. This outperforms the zero-shot CoT prompted and retrieval-augmented GPT-3 by +1.9%.

5.4 INFORMATION RETRIEVAL

We tested whether retrievers trained using VOD could be applied to information retrieval. We benchmark deep retrievers against the FindZebra API⁶ based on the set of FindZebra queries and corpus. We applied the VOD retriever trained to use question-answer MedMCQA pairs $[\mathbf{q}; \mathbf{a}]$ as input and tested an additional model trained using distillation to use queries \mathbf{q} as input. We also evaluated a hybrid retriever with score $f_\theta^{\text{VOD+BM25}}(\mathbf{d}, \mathbf{q}) := f_\theta(\mathbf{q}, \mathbf{d}) + \tau^{-1} \text{BM25}(\mathbf{q}, \mathbf{d})$ where $\tau = 5$.

Task-specific distillation We use the VOD retriever trained using question-answer pairs as a teacher to train an additional student BioLinkBERT model using questions only. This corresponds to applying knowledge distillation with the loss:

$$L_{\text{DISTILL.}} = D_{\text{KL}}(r_\phi(\mathbf{d} \mid [\mathbf{q}; \mathbf{a}_*]) \parallel p_\theta(\mathbf{d} \mid \mathbf{q})).$$

Metrics We reduced the retrieved passages by article identifier and recorded the rank of the first article linked to a CUI (disease concept) that matches the labels. We report the mean reciprocal rank (MRR) and the fraction of queries for which the correct article is returned in the top 20.

Table 6: Retrieval performances on the FindZebra benchmark for a BioLinkBERT retriever trained using VOD on MedMCQA and one trained using task-specific distillation, with and without coupling with a BM25 score during evaluation.

Method	Distillation	MRR	Hit@20
VOD	✗	27.8	56.9
VOD	✓	31.7	58.1
VOD + BM25	✓	38.9	64.1
BM25	—	26.4	48.4
FindZebra API	—	30.1	59.3

Performances The FindZebra API implements an advanced custom BM25 score (Dragusin et al., 2013) which powers a specialized search engine utilized by many medical professionals. Nonetheless, a retriever trained using VOD on the MedMCQA dataset is competitive with the API (31.8 MRR for VOD, 30.1 MRR for the API). Coupling the distilled retriever with a simple BM25 baseline gave the best performance with an MRR of 38.9. We found that task-specific distillation was beneficial when applying multiple-choice ODQA retrievers to information retrieval: the task-specific distilled retriever scored 3.9 MRR points above the reference retriever.

Retriever samples In Table 7, we report retrieved top-1 passages for the distilled retriever (two successes and two failures). We found that search results were overall relevant and that terms from the input medical description were utilized and matched beyond simple keyword searches. Nonetheless, the deep retriever often fails when queried with longer comma-separated lists of keywords, as shown in row #4. We speculate that the gap between the training and inference tasks remains large.

6 CONCLUSION

We have introduced VOD, a probabilistic framework for end-to-end training of retrieval augmented models. VOD models the retrieval process explicitly using a target-aware posterior, allowing tractable and consistent estimation of a marginal log-likelihood lower bound. We applied VOD to end-to-end training of multiple-choice ODQA models and scored state-of-the-art results on two datasets. Furthermore, we introduced a medical information retrieval benchmark, which we used to showcase that retrievers trained with VOD can be competitive with industrial search engines.

Although we only applied the framework to the multiple-choice setting with a static approximate posterior, VOD can be applied to a wide range of retrieval-augmented models. Alternatively, the approximate posterior can be learned jointly. We hope our view of retrieval-augmented modelling will spark further interest in designing and training likelihood-based models.

ACKNOWLEDGMENTS

OW’s work was funded in part by the Novo Nordisk Foundation through the Center for Basic Machine Learning Research in Life Science (NNF20OC0062606). OW acknowledges support from the Pioneer Centre for AI, DNRF grant number P1.

⁶<https://www.findzebra.com/api/>

Table 7: Top-1 passages retrieved for a selection of FindZebra queries with their annotated answer CUIs and the rank of the first matching article for VOD and the FindZebra API. We showcase the retriever model trained with task-specific distillation and without BM25 coupling (MRR 31.7). We highlight terms from the queries and passages relevant to each other.

#	Query	Passage
1	Q: widespread musculoskeletal pain for more than 6 months and point tenderness in at least 11 of 18 defined anatomical sites A: Fibromyalgia (C0016053) Hit rank: VODBERT=1, FZAPI=1	<i>Fibromyalgia</i> . (...) for IL-1 receptor antagonist, IL-6 and IL-8. Diagnosis The location of the nine paired tender points that comprise the 1990 American College of Rheumatology criteria for fibromyalgia There is no single pathological feature, laboratory finding or biomarker that can diagnose fibromyalgia and there is debate over what should be considered diagnostic criteria and whether an objective diagnosis is possible. In most cases, people with fibromyalgia symptoms may have laboratory test results that appear normal and many of their symptoms may mimic those of other rheumatic conditions such as arthritis or osteoporosis. The most widely accepted set of classification criteria for research purposes was elaborated in 1990 by the Multicenter Criteria Committee of the American College of Rheumatology. These criteria, which are known informally as "the ACR 1990", define fibromyalgia according to the presence of the following criteria: A history of widespread pain lasting more than three months – affecting all four quadrants of the body, i.e., both sides, and above and below the waist. Tender points – there (...)
2	Q: diagnosis for dementing syndrome characterized primarily by impairment of interpersonal and executive function A: Frontotemporal dementia (C0338451) Hit rank: VODBERT=1, FZAPI=8	<i>Frontotemporal dementia</i> . (FTDs) are a group of neurodegenerative disorders associated with shrinking of the frontal and temporal anterior lobes of the brain. Symptoms include marked changes in social behavior and personality, and/or problems with language. People with behavior changes may have disinhibition (with socially inappropriate behavior), apathy and loss of empathy, hyperorality (eating excessive amounts of food or attempting to consume inedible things), agitation, compulsive behavior, and various other changes. Examples of problems with language include difficulty speaking or understanding speech. Some people with FTD also develop a motor syndrome such as parkinsonism or motor neuron disease (which may be associated with various additional symptoms). There is a strong genetic component to FTDs. It sometimes follows an autosomal dominant inheritance pattern, or sometimes there is a general family history of dementia or psychiatric disorders. The three main genes responsible for familial FTD are MAPT, GRN, and C9orf72. However, the (...)
3	Q: syndrome characterized by cough, reversible wheezing, and peripheral blood eosinophilia A: Asthma (C0004096), Reactive airway disease (C3714497) Hit rank: VODBERT=72, FZAPI=11	<i>Löffler's syndrome</i> . (...) a parasitic infection such as irritable bowel syndrome, abdominal pain and cramping, skin rashes and fatigue. Löffler's syndrome itself will cause difficulty breathing, coughing as well as a fever. Contents 1 Diagnosis 2 Prevention 3 Epidemiology 4 History 5 See also 6 References 7 External links Diagnosis The diagnosis of Löffler's syndrome can be challenging, as the diagnostic criteria can be vague and consistent with a multitude of diseases or conditions. The disease's developmental trajectory is mostly unknown. Upon examination of symptoms, a doctor will likely request a chest x-ray looking for migratory pulmonary infiltrate, and blood testing, to confirm a diagnosis. Symptoms tend to be brief, but can range from mild to severe and include: fever, vomiting, increased respirations or difficulty breathing, cough, wheeze, and rash . Symptoms typically follow an exposure to allergens or certain drugs, and last approximately two weeks. Eosinophilia is the main feature of diagnostic (...)
4	Q: 5 year old, boy, congenital malformations, malformations of the hands and feet, bilateral strabismus, small tongue, impaired coordination, expressionless face, prominent forehead, depressed nasal bridge, hypoplastic thumbs, bilateral adactyly of the feet, short stature, severe myopia A: Mobius Syndrome (C0221060), Mobius II syndrome (C0853240) Hit rank: VODBERT=∞, FZAPI=1	<i>Achondroplasia</i> . (...) hypochondroplasia, but the features of achondroplasia tend to be more severe. All people with achondroplasia have short stature. The average height of an adult male with achondroplasia is 131 centimeters (4 feet, 4 inches), and the average height for adult females is 124 centimeters (4 feet, 1 inch). Characteristic features of achondroplasia include an average-size trunk, short arms and legs with particularly short upper arms and thighs, limited range of motion at the elbows, and an enlarged head (macrocephaly) with a prominent forehead . Fingers are typically short and the ring finger and middle finger may diverge, giving the hand a three-pronged (trident) appearance. People with achondroplasia are generally of normal intelligence. Health problems commonly associated with achondroplasia include episodes in which breathing slows or stops for short periods (apnea, obesity, (...)

REFERENCES

Olivier Bodenreider. The unified medical language system (UMLS): integrating biomedical terminology. *Nucleic acids research*, 32(Database issue):D267–70, January 2004. ISSN 0305-1048, 1362-4962. doi: 10.1093/nar/gkh061.

Sebastian Borgeaud, Arthur Mensch, Jordan Hoffmann, Trevor Cai, Eliza Rutherford, Katie Millican, George van den Driessche, Jean-Baptiste Lespiau, Bogdan Damoc, Aidan Clark, Diego de Las Casas, Aurelia Guy, Jacob Menick, Roman Ring, Tom Hennigan, Saffron Huang, Loren Maggiore, Chris Jones, Albin Cassirer, Andy Brock, Michela Paganini, Geoffrey Irving, Oriol Vinyals, Simon Osindero, Karen Simonyan, Jack W Rae, Erich Elsen, and Laurent Sifre. Improving language models by retrieving from trillions of tokens. December 2021.

T Brown, B Mann, N Ryder, and others. Language models are few-shot learners. *Advances in neural information processing systems*, 2020. ISSN 1049-5258.

Yuri Burda, Roger Grosse, and Ruslan Salakhutdinov. Importance weighted autoencoders. September 2015.

Danqi Chen, Adam Fisch, Jason Weston, and Antoine Bordes. Reading wikipedia to answer Open-Domain questions. March 2017.

Aakanksha Chowdhery, Sharan Narang, Jacob Devlin, Maarten Bosma, Gaurav Mishra, Adam Roberts, Paul Barham, Hyung Won Chung, Charles Sutton, Sebastian Gehrmann, Parker Schuh, Kensen Shi, Sasha Tsvyashchenko, Joshua Maynez, Abhishek Rao, Parker Barnes, Yi Tay, Noam Shazeer, Vinodkumar Prabhakaran, Emily Reif, Nan Du, Ben Hutchinson, Reiner Pope, James Bradbury, Jacob Austin, Michael Isard, Guy Gur-Ari, Pengcheng Yin, Toju Duke, Anselm Levskaya, Sanjay Ghemawat, Sunipa Dev, Henryk Michalewski, Xavier Garcia, Vedant Misra, Kevin Robinson, Liam Fedus, Denny Zhou, Daphne Ippolito, David Luan, Hyeontaek Lim, Barret Zoph, Alexander Spiridonov, Ryan Sepassi, David Dohan, Shivani Agrawal, Mark Omernick, Andrew M Dai, Thanumalayan Sankaranarayana Pillai, Marie Pellat, Aitor Lewkowycz, Erica Moreira, Rewon Child, Oleksandr Polozov, Katherine Lee, Zongwei Zhou, Xuezhi Wang, Brennan Saeta, Mark Diaz, Orhan Firat, Michele Catasta, Jason Wei, Kathy Meier-Hellstern, Douglas Eck, Jeff Dean, Slav Petrov, and Noah Fiedel. PaLM: Scaling language modeling with pathways. April 2022.

Chris Cremer, Xuechen Li, and David Duvenaud. Inference suboptimality in variational autoencoders. January 2018.

Jacob Devlin, Ming-Wei Chang, Kenton Lee, and Kristina Toutanova. BERT: Pre-training of deep bidirectional transformers for language understanding. October 2018.

Radu Dragusin, Paula Petcu, Christina Lioma, Birger Larsen, Henrik L Jørgensen, Ingemar J Cox, Lars Kai Hansen, Peter Ingwersen, and Ole Winther. FindZebra: A search engine for rare diseases. *International journal of medical informatics*, 82(6):528–538, June 2013. ISSN 1386-5056. doi: 10.1016/j.ijmedinf.2013.01.005.

Nick Duffield, Carsten Lund, and Mikkel Thorup. Priority sampling for estimation of arbitrary subset sums. *Journal of the ACM*, 54(6):32–es, December 2007. ISSN 0004-5411. doi: 10.1145/1314690.1314696.

Víctor Elvira and Luca Martino. Advances in importance sampling. February 2021.

Falcon. PyTorch lightning. *GitHub. Note*: <https://github.com/PyTorchLightning/pytorch-lightning>.

William Fedus, Barret Zoph, and Noam Shazeer. Switch transformers: Scaling to trillion parameter models with simple and efficient sparsity, 2021.

Will Grathwohl, Dami Choi, Yuhuai Wu, Geoffrey Roeder, and David Duvenaud. Backpropagation through the void: Optimizing control variates for black-box gradient estimation. October 2017.

Yu Gu, Robert Tinn, Hao Cheng, Michael Lucas, Naoto Usuyama, Xiaodong Liu, Tristan Naumann, Jianfeng Gao, and Hoifung Poon. Domain-Specific language model pretraining for biomedical natural language processing. *ACM Trans. Comput. Healthcare*, 3(1):1–23, October 2021. ISSN 2691-1957. doi: 10.1145/3458754.

Kelvin Guu, Kenton Lee, Zora Tung, Panupong Pasupat, and Mingwei Chang. Retrieval augmented language model Pre-Training. In Hal Daumé III and Aarti Singh (eds.), *Proceedings of the 37th International Conference on Machine Learning*, volume 119 of *Proceedings of Machine Learning Research*, pp. 3929–3938. PMLR, 2020.

G E Hinton, P Dayan, B J Frey, and R M Neal. The “wake-sleep” algorithm for unsupervised neural networks. *Science*, 268(5214):1158–1161, May 1995. ISSN 0036-8075. doi: 10.1126/science.7761831.

Jordan Hoffmann, Sebastian Borgeaud, Arthur Mensch, Elena Buchatskaya, Trevor Cai, Eliza Rutherford, Diego de Las Casas, Lisa Anne Hendricks, Johannes Welbl, Aidan Clark, Tom Hennigan, Eric Noland, Katie Millican, George van den Driessche, Bogdan Damoc, Aurelia Guy, Simon Osindero, Karen Simonyan, Erich Elsen, Jack W Rae, Oriol Vinyals, and Laurent Sifre. Training Compute-Optimal large language models, 2022.

Gautier Izacard and Edouard Grave. Distilling knowledge from reader to retriever for question answering. December 2020a.

Gautier Izacard and Edouard Grave. Leveraging passage retrieval with generative models for open domain question answering. July 2020b.

Gautier Izacard, Mathilde Caron, Lucas Hosseini, Sebastian Riedel, Piotr Bojanowski, Armand Joulin, and Edouard Grave. Unsupervised dense information retrieval with contrastive learning. December 2021.

Gautier Izacard, Patrick Lewis, Maria Lomeli, Lucas Hosseini, Fabio Petroni, Timo Schick, Jane Dwivedi-Yu, Armand Joulin, Sebastian Riedel, and Edouard Grave. Few-shot learning with retrieval augmented language models. August 2022.

Di Jin, Eileen Pan, Nassim Oufattolle, Wei-Hung Weng, Hanyi Fang, and Peter Szolovits. What disease does this patient have? a large-scale open domain question answering dataset from medical exams. *APPS. Applied Sciences*, 11(14):6421, July 2021. ISSN 1454-5101, 2076-3417. doi: 10.3390/app11146421.

Jeff Johnson, Matthijs Douze, and Herve Jegou. Billion-scale similarity search with GPUs. *IEEE transactions on big data*, 7(3):535–547, July 2021. ISSN 2332-7790, 2372-2096. doi: 10.1109/tbdata.2019.2921572.

Michael I Jordan, Zoubin Ghahramani, Tommi S Jaakkola, and Lawrence K Saul. An introduction to variational methods for graphical models. *Machine learning*, 37(2):183–233, November 1999. ISSN 0885-6125, 1573-0565. doi: 10.1023/A:1007665907178.

Vladimir Karpukhin, Barlas Oğuz, Sewon Min, Patrick Lewis, Ledell Wu, Sergey Edunov, Danqi Chen, and Wen-Tau Yih. Dense passage retrieval for Open-Domain question answering. April 2020.

Omar Khattab and Matei Zaharia. ColBERT: Efficient and effective passage search via contextualized late interaction over BERT. In *Proceedings of the 43rd International ACM SIGIR Conference on Research and Development in Information Retrieval*, pp. 39–48. Association for Computing Machinery, New York, NY, USA, July 2020. ISBN 9781450380164. doi: 10.1145/3397271.3401075.

Omar Khattab, Christopher Potts, and Matei Zaharia. Relevance-guided supervision for OpenQA with ColBERT. *Transactions of the Association for Computational Linguistics*, 9:929–944, September 2021. ISSN 2307-387X. doi: 10.1162/tacl_a_00405.

Takeshi Kojima, Shixiang Shane Gu, Machel Reid, Yutaka Matsuo, and Yusuke Iwasawa. Large language models are Zero-Shot reasoners. May 2022.

Wouter Kool, Herke Van Hoof, and Max Welling. Stochastic beams and where to find them: The Gumbel-Top-k trick for sampling sequences without replacement. In Kamalika Chaudhuri and Ruslan Salakhutdinov (eds.), *Proceedings of the 36th International Conference on Machine Learning*, volume 97 of *Proceedings of Machine Learning Research*, pp. 3499–3508. PMLR, 2019a.

Wouter Kool, Herke van Hoof, and Max Welling. Buy 4 REINFORCE samples, get a baseline for free! March 2019b.

Hugo Laurençon, Lucile Saulnier, Thomas Wang, Christopher Akiki, Albert Villanova del Moral, Teven Le Scao, Leandro Von Werra, Chenghao Mou, Eduardo González Ponferrada, Huu Nguyen, Jörg Frohberg, Mario Šaško, Quentin Lhoest, Angelina McMillan-Major, Gérard Dupont, Stella Biderman, Anna Rogers, Loubna Ben allal, Francesco De Toni, Giada Pistilli, Olivier Nguyen, Somaieh Nikpoor, Maraim Masoud, Pierre Colombo, Javier de la Rosa, Paulo Villegas, Tristan Thrush, Shayne Longpre, Sebastian Nagel, Leon Weber, Manuel Romero Muñoz, Jian Zhu, Daniel Van Strien, Zaid Alyafeai, Khalid Almubarak, Vu Minh Chien, Itziar Gonzalez-Dios, Aitor Soroa, Kyle Lo, Manan Dey, Pedro Ortiz Suarez, Aaron Gokaslan, Shamik Bose, David Ifeoluwa Adelani, Long Phan, Ian Yu, Suhas Pai, Violette Lepercq, Suzana Ilic, Margaret Mitchell, Sasha Luccioni, and Yacine Jernite. The BigScience corpus a 1.6TB composite multilingual dataset. June 2022.

Angeliki Lazaridou, Elena Gribovskaya, Wojciech Stokowiec, and Nikolai Grigorev. Internet-augmented language models through few-shot prompting for open-domain question answering. March 2022.

Tuan Anh Le, Adam R Kosiorek, N Siddharth, Yee Whye Teh, and Frank Wood. Revisiting reweighted Wake-Sleep for models with stochastic control flow. May 2018.

Jinhyuk Lee, Wonjin Yoon, Sungdong Kim, Donghyeon Kim, Sunkyu Kim, Chan Ho So, and Jaewoo Kang. BioBERT: a pre-trained biomedical language representation model for biomedical text mining. *Bioinformatics*, 36(4):1234–1240, February 2020. ISSN 1367-4803, 1367-4811. doi: 10.1093/bioinformatics/btz682.

Kenton Lee, Ming-Wei Chang, and Kristina Toutanova. Latent retrieval for weakly supervised open-domain question answering. In *Proceedings of the 57th Annual Meeting of the Association for Computational Linguistics*, pp. 6086–6096, Florence, Italy, July 2019. Association for Computational Linguistics. doi: 10.18653/v1/P19-1612.

Mike Lewis, Yinhan Liu, Naman Goyal, Marjan Ghazvininejad, Abdelrahman Mohamed, Omer Levy, Ves Stoyanov, and Luke Zettlemoyer. BART: Denoising Sequence-to-Sequence pre-training for natural language generation, translation, and comprehension. October 2019.

Patrick Lewis, Ethan Perez, Aleksandra Piktus, Fabio Petroni, Vladimir Karpukhin, Naman Goyal, Heinrich Kütter, Mike Lewis, Wen-Tau Yih, Tim Rocktäschel, Sebastian Riedel, and Douwe Kiela. Retrieval-Augmented generation for Knowledge-Intensive NLP tasks. In H Larochelle, M Ranzato, R Hadsell, M F Balcan, and H Lin (eds.), *Advances in Neural Information Processing Systems*, volume 33, pp. 9459–9474. Curran Associates, Inc., 2020.

Yingzhen Li and Richard E Turner. Rényi divergence variational inference. In D D Lee, M Sugiyama, U V Luxburg, I Guyon, and R Garnett (eds.), *Advances in Neural Information Processing Systems* 29, pp. 1073–1081. Curran Associates, Inc., 2016.

Opher Lieber, Or Sharir, Barak Lenz, and Yoav Shoham. Jurassic-1: Technical details and evaluation. Technical report, AI21 Labs, August 2021.

Valentin Liévin, Andrea Dittadi, Anders Christensen, and Ole Winther. Optimal variance control of the Score-Function gradient estimator for Importance-Weighted bounds. *Advances in neural information processing systems*, 33:16591–16602, 2020. ISSN 1049-5258.

Valentin Liévin, Christoffer Egeberg Hother, and Ole Winther. Can large language models reason about medical questions? July 2022.

Vaden Masrani, Tuan Anh Le, and Frank Wood. The thermodynamic variational objective. June 2019.

Andriy Mnih and Karol Gregor. Neural variational inference and learning in belief networks. January 2014.

Andriy Mnih and Danilo J Rezende. Variational inference for monte carlo objectives. February 2016.

Ankit Pal, Logesh Kumar Umapathi, and Malaikannan Sankarasubbu. MedMCQA: A large-scale Multi-Subject Multi-Choice dataset for medical domain question answering. In Gerardo Flores, George H Chen, Tom Pollard, Joyce C Ho, and Tristan Naumann (eds.), *Proceedings of the Conference on Health, Inference, and Learning*, volume 174 of *Proceedings of Machine Learning Research*, pp. 248–260. PMLR, 2022.

Ashwin Paranjape, Omar Khattab, Christopher Potts, Matei Zaharia, and Christopher D Manning. Hindsight: Posterior-guided training of retrievers for improved open-ended generation. October 2021.

Paszke, Gross, Massa, Lerer, and others. Pytorch: An imperative style, high-performance deep learning library. *Advances in neural information processing systems*, 2019. ISSN 1049-5258.

Yingqi Qu, Yuchen Ding, Jing Liu, Kai Liu, Ruiyang Ren, Wayne Xin Zhao, Daxiang Dong, Hua Wu, and Haifeng Wang. RocketQA: An optimized training approach to dense passage retrieval for Open-Domain question answering. In *Proceedings of the 2021 Conference of the North American Chapter of the Association for Computational Linguistics: Human Language Technologies*, pp. 5835–5847, Online, June 2021. Association for Computational Linguistics. doi: 10.18653/v1/2021.naacl-main.466.

A Radford, K Narasimhan, T Salimans, and I Sutskever. Improving language understanding by generative pre-training. *cs.ubc.ca*, 2018.

Jack W Rae, Sebastian Borgeaud, Trevor Cai, Katie Millican, Jordan Hoffmann, Francis Song, John Aslanides, Sarah Henderson, Roman Ring, Susannah Young, Eliza Rutherford, Tom Hennigan, Jacob Menick, Albin Cassirer, Richard Powell, George van den Driessche, Lisa Anne Hendricks, Maribeth Rauh, Po-Sen Huang, Amelia Glaese, Johannes Welbl, Sumanth Dathathri, Saffron Huang, Jonathan Uesato, John Mellor, Irina Higgins, Antonia Creswell, Nat McAleese, Amy Wu, Erich Elsen, Siddhant Jayakumar, Elena Buchatskaya, David Budden, Esme Sutherland, Karen Simonyan, Michela Paganini, Laurent Sifre, Lena Martens, Xiang Lorraine Li, Adhiguna Kuncoro, Aida Nematzadeh, Elena Gribovskaya, Domenic Donato, Angeliki Lazaridou, Arthur Mensch, Jean-Baptiste Lespiau, Maria Tsimpoukelli, Nikolai Grigorev, Doug Fritz, Thibault Sottiaux, Mantas Pajarskas, Toby Pohlen, Zhitao Gong, Daniel Toyama, Cyprien de Masson d'Autume, Yujia Li, Tayfun Terzi, Vladimir Mikulik, Igor Babuschkin, Aidan Clark, Diego de Las Casas, Aurelia Guy, Chris Jones, James Bradbury, Matthew Johnson, Blake Hechtman, Laura Weidinger, Iason Gabriel, William Isaac, Ed Lockhart, Simon Osindero, Laura Rimell, Chris Dyer, Oriol Vinyals, Kareem Ayoub, Jeff Stanway, Lorrayne Bennett, Demis Hassabis, Koray Kavukcuoglu, and Geoffrey Irving. Scaling language models: Methods, analysis & insights from training gopher. December 2021.

Devendra Sachan, Mostafa Patwary, Mohammad Shoeybi, Neel Kant, Wei Ping, William L Hamilton, and Bryan Catanzaro. End-to-End training of neural retrievers for Open-Domain question answering, 2021a.

Devendra Singh Sachan, Siva Reddy, William Hamilton, Chris Dyer, and Dani Yogatama. End-to-End training of Multi-Document reader and retriever for Open-Domain question answering. *NeurIPS*, 2021b.

Shaden Smith, Mostafa Patwary, Brandon Norick, Patrick LeGresley, Samyam Rajbhandari, Jared Casper, Zhun Liu, Shrimai Prabhumoye, George Zerveas, Vijay Korthikanti, Elton Zhang, Rewon Child, Reza Yazdani Aminabadi, Julie Bernauer, Xia Song, Mohammad Shoeybi, Yuxiong He, Michael Houston, Saurabh Tiwary, and Bryan Catanzaro. Using DeepSpeed and megatron to train Megatron-Turing NLG 530b, a Large-Scale generative language model, 2022.

Aarohi Srivastava, Abhinav Rastogi, Abhishek Rao, Abu Awal Md Shoeb, Abubakar Abid, Adam Fisch, Adam R Brown, Adam Santoro, Aditya Gupta, Adrià Garriga-Alonso, Agnieszka Kluska, Aitor Lewkowycz, Akshat Agarwal, Alethea Power, Alex Ray, Alex Warstadt, Alexander W Kocurek, Ali Safaya, Ali Tazarv, Alice Xiang, Alicia Parrish, Allen Nie, Aman Hussain, Amanda Askell, Amanda Dsouza, Ambrose Slone, Ameet Rahane, Anantharaman S Iyer, Anders Andreassen, Andrea Madotto, Andrea Santilli, Andreas Stuhlmüller, Andrew Dai, Andrew La, Andrew Lampinen, Andy Zou, Angela Jiang, Angelica Chen, Anh Vuong, Animesh Gupta, Anna Gottardi, Antonio Norelli, Anu Venkatesh, Arash Gholamidavoodi, Arfa Tabassum, Arul Menezes, Arun

Kirubarajan, Asher Mullokandov, Ashish Sabharwal, Austin Herrick, Avia Efrat, Aykut Erdem, Ayla Karakaş, B Ryan Roberts, Bao Sheng Loe, Barret Zoph, Bartłomiej Bojanowski, Batuhan Özyurt, Behnam Hedayatnia, Behnam Neyshabur, Benjamin Inden, Benno Stein, Berk Ekmekci, Bill Yuchen Lin, Blake Howald, Cameron Diao, Cameron Dour, Catherine Stinson, Cedrick Aragueta, César Ferri Ramírez, Chandan Singh, Charles Rathkopf, Chenlin Meng, Chitta Baral, Chiyu Wu, Chris Callison-Burch, Chris Waites, Christian Voigt, Christopher D Manning, Christopher Potts, Cindy Ramirez, Clara E Rivera, Clemencia Siro, Colin Raffel, Courtney Ashcraft, Cristina Garbacea, Damien Sileo, Dan Garrette, Dan Hendrycks, Dan Kilman, Dan Roth, Daniel Freeman, Daniel Khashabi, Daniel Levy, Daniel Moseguí González, Danielle Perszyk, Danny Hernandez, Danqi Chen, Daphne Ippolito, Dar Gilboa, David Dohan, David Drakard, David Jurgens, Debajyoti Datta, Deep Ganguli, Denis Emelin, Denis Kleyko, Deniz Yuret, Derek Chen, Derek Tam, Dieuwke Hupkes, Diganta Misra, Dilyar Buzan, Dimitri Coelho Mollo, Diyi Yang, Dong-Ho Lee, Ekaterina Shutova, Ekin Dogus Cubuk, Elad Segal, Eleanor Hagerman, Elizabeth Barnes, Elizabeth Donoway, Ellie Pavlick, Emanuele Rodola, Emma Lam, Eric Chu, Eric Tang, Erkut Erdem, Ernie Chang, Ethan A Chi, Ethan Dyer, Ethan Jerzak, Ethan Kim, Eunice Engefu Manyasi, Evgenii Zheltonozhskii, Fanyue Xia, Fatemeh Siar, Fernando Martínez-Plumed, Francesca Happé, Francois Chollet, Frieda Rong, Gaurav Mishra, Genta Indra Winata, Gerard de Melo, Germán Kruszewski, Giambattista Parascandolo, Giorgio Mariani, Gloria Wang, Gonzalo Jaimovich-López, Gregor Betz, Guy Gur-Ari, Hana Galijasevic, Hannah Kim, Hannah Rashkin, Hannaneh Hajishirzi, Harsh Mehta, Hayden Bogar, Henry Shevlin, Hinrich Schütze, Hiromu Yakura, Hongming Zhang, Hugh Mee Wong, Ian Ng, Isaac Noble, Jaap Jumelet, Jack Geissinger, Jackson Kernion, Jacob Hilton, Jaehoon Lee, Jaime Fernández Fisac, James B Simon, James Koppel, James Zheng, James Zou, Jan Kocoń, Jana Thompson, Jared Kaplan, Jarema Radom, Jascha Sohl-Dickstein, Jason Phang, Jason Wei, Jason Yosinski, Jekaterina Novikova, Jelle Bosscher, Jennifer Marsh, Jeremy Kim, Jeroen Taal, Jesse Engel, Jesujoba Alabi, Jiacheng Xu, Jiaming Song, Jillian Tang, Joan Waweru, John Burden, John Miller, John U Balis, Jonathan Berant, Jörg Frohberg, Jos Rozen, Jose Hernandez-Orallo, Joseph Boudeman, Joseph Jones, Joshua B Tenenbaum, Joshua S Rule, Joyce Chua, Kamil Kandlerz, Karen Livescu, Karl Krauth, Karthik Gopalakrishnan, Katerina Ignatyeva, Katja Markert, Kaustubh D Dhole, Kevin Gimpel, Kevin Omondi, Kory Mathewson, Kristen Chiafulla, Ksenia Shkaruta, Kumar Shridhar, Kyle McDonell, Kyle Richardson, Laria Reynolds, Leo Gao, Li Zhang, Liam Dugan, Lianhui Qin, Lidia Contreras-Ochando, Louis-Philippe Morency, Luca Moschella, Lucas Lam, Lucy Noble, Ludwig Schmidt, Luheng He, Luis Oliveros Colón, Luke Metz, Lütfi Kerem Şenel, Maarten Bosma, Maarten Sap, Maartje ter Hoeve, Maheen Farooqi, Manaal Faruqui, Mantas Mazeika, Marco Baturan, Marco Marelli, Marco Maru, Maria Jose Ramírez Quintana, Marie Tolkiehn, Mario Giulianelli, Martha Lewis, Martin Potthast, Matthew L Leavitt, Matthias Hagen, Mátyás Schubert, Medina Orduna Baitemirova, Melody Arnaud, Melvin McElrath, Michael A Yee, Michael Cohen, Michael Gu, Michael Ivanitskiy, Michael Starritt, Michael Strube, Michał Swędrowski, Michele Bevilacqua, Michihiro Yasunaga, Mihir Kale, Mike Cain, Mimee Xu, Mirac Suzgun, Mo Tiwari, Mohit Bansal, Moin Aminnaseri, Mor Geva, Mozhdeh Gheini, Mukund Varma T, Nanyun Peng, Nathan Chi, Nayeon Lee, Neta Gur-Ari Krakover, Nicholas Cameron, Nicholas Roberts, Nick Doiron, Nikita Nangia, Niklas Deckers, Niklas Muennighoff, Nitish Shirish Keskar, Niveditha S Iyer, Noah Constant, Noah Fiedel, Nuan Wen, Oliver Zhang, Omar Agha, Omar Elbaghdadi, Omer Levy, Owain Evans, Pablo Antonio Moreno Casares, Parth Doshi, Pascale Fung, Paul Pu Liang, Paul Vicol, Pegah Alipoormolabashi, Peiyuan Liao, Percy Liang, Peter Chang, Peter Eckersley, Phu Mon Htut, Pinyu Hwang, Piotr Miłkowski, Piyush Patil, Pouya Pezeshkpour, Priti Oli, Qiaozhu Mei, Qing Lyu, Qinlang Chen, Rabin Banjade, Rachel Etta Rudolph, Raefer Gabriel, Rahel Habacker, Ramón Risco Delgado, Raphaël Millière, Rhythm Garg, Richard Barnes, Rif A Saurous, Riku Arakawa, Robbe Raymaekers, Robert Frank, Rohan Sikand, Roman Novak, Roman Sitelew, Ronan LeBras, Rosanne Liu, Rowan Jacobs, Rui Zhang, Ruslan Salakhutdinov, Ryan Chi, Ryan Lee, Ryan Stovall, Ryan Teehan, Rylan Yang, Sahib Singh, Saif M Mohammad, Sajant Anand, Sam Dillavou, Sam Shleifer, Sam Wiseman, Samuel Gruetter, Samuel R Bowman, Samuel S Schoenholz, Sanghyun Han, Sanjeev Kwatra, Sarah A Rous, Sarik Ghazarian, Sayan Ghosh, Sean Casey, Sebastian Bischoff, Sebastian Gehrmann, Sebastian Schuster, Sepideh Sadeghi, Shadi Hamdan, Sharon Zhou, Shashank Srivastava, Sherry Shi, Shikhar Singh, Shima Asaadi, Shixiang Shane Gu, Shubh Pachchigar, Shubham Toshniwal, Shyam Upadhyay, Shyamolima, Debnath, Siamak Shakeri, Simon Thormeyer, Simone Melzi, Siva Reddy, Sneha Priscilla Makini, Soo-Hwan Lee, Spencer Torene, Sriharsha Hatwar, Stanislas Dehaene, Stefan Divic, Stefano Ermon, Stella Biderman, Stephanie Lin, Stephen Prasad, Steven T Piantadosi, Stuart M Shieber, Summer Misherghi, Svetlana Kiritchenko, Swaroop Mishra, Tal Linzen, Tal Schuster, Tao Li,

Tao Yu, Tariq Ali, Tatsu Hashimoto, Te-Lin Wu, Théo Desbordes, Theodore Rothschild, Thomas Phan, Tianle Wang, Tiberius Nkinyili, Timo Schick, Timofei Kornev, Timothy Telleen-Lawton, Titus Tunduny, Tobias Gerstenberg, Trenton Chang, Trishala Neeraj, Tushar Khot, Tyler Shultz, Uri Shaham, Vedant Misra, Vera Demberg, Victoria Nyamai, Vikas Raunak, Vinay Ramasesh, Vinay Uday Prabhu, Vishakh Padmakumar, Vivek Srikanth, William Fedus, William Saunders, William Zhang, Wout Vossen, Xiang Ren, Xiaoyu Tong, Xinran Zhao, Xinyi Wu, Xudong Shen, Yadollah Yaghoobzadeh, Yair Lakretz, Yangqiu Song, Yasaman Bahri, Yejin Choi, Yichi Yang, Yiding Hao, Yifu Chen, Yonatan Belinkov, Yu Hou, Yufang Hou, Yuntao Bai, Zachary Seid, Zhuoye Zhao, Zijian Wang, Zijie J Wang, Zirui Wang, and Ziyi Wu. Beyond the imitation game: Quantifying and extrapolating the capabilities of language models, 2022.

Romal Thoppilan, Daniel De Freitas, Jamie Hall, Noam Shazeer, Apoorv Kulshreshtha, Heng-Tze Cheng, Alicia Jin, Taylor Bos, Leslie Baker, Yu Du, Yaguang Li, Hongrae Lee, Huaixiu Steven Zheng, Amin Ghafouri, Marcelo Menegali, Yanping Huang, Maxim Krikun, Dmitry Lepikhin, James Qin, Dehao Chen, Yuanzhong Xu, Zhifeng Chen, Adam Roberts, Maarten Bosma, Vincent Zhao, Yanqi Zhou, Chung-Ching Chang, Igor Krivokon, Will Rusch, Marc Pickett, Pranesh Srinivasan, Laichee Man, Kathleen Meier-Hellstern, Meredith Ringel Morris, Tulsee Doshi, Renelito Delos Santos, Toju Duke, Johnny Soraker, Ben Zevenbergen, Vinodkumar Prabhakaran, Mark Diaz, Ben Hutchinson, Kristen Olson, Alejandra Molina, Erin Hoffman-John, Josh Lee, Lora Aroyo, Ravi Rajakumar, Alena Butryna, Matthew Lamm, Viktoriya Kuzmina, Joe Fenton, Aaron Cohen, Rachel Bernstein, Ray Kurzweil, Blaise Aguera-Arcas, Claire Cui, Marian Croak, Ed Chi, and Quoc Le. LaMDA: Language models for dialog applications. January 2022.

George Tucker, Andriy Mnih, Chris J Maddison, John Lawson, and Jascha Sohl-Dickstein. REBAR: Low-variance, unbiased gradient estimates for discrete latent variable models. In I Guyon, U V Luxburg, S Bengio, H Wallach, R Fergus, S Vishwanathan, and R Garnett (eds.), *Advances in Neural Information Processing Systems 30*, pp. 2627–2636. Curran Associates, Inc., 2017.

Aaron van den Oord, Oriol Vinyals, and Koray Kavukcuoglu. Neural discrete representation learning. November 2017.

Ashish Vaswani, Noam Shazeer, Niki Parmar, Jakob Uszkoreit, Llion Jones, Aidan N Gomez, Łukasz Kaiser, and Illia Polosukhin. Attention is all you need. *Advances in neural information processing systems*, 30, 2017. ISSN 1049-5258.

Tim Vieira. Estimating means in a finite universe. <https://timvieira.github.io/blog/post/2017/07/03/estimating-means-in-a-finite-universe/>, 2017. Accessed: 2022-NA-NA.

Sohee Yang and Minjoon Seo. Is retriever merely an approximator of reader? October 2020.

Michihiro Yasunaga, Jure Leskovec, and Percy Liang. LinkBERT: Pretraining language models with document links. March 2022.

Susan Zhang, Stephen Roller, Naman Goyal, Mikel Artetxe, Moya Chen, Shuhui Chen, Christopher Dewan, Mona Diab, Xian Li, Xi Victoria Lin, Todor Mihaylov, Myle Ott, Sam Shleifer, Kurt Shuster, Daniel Simig, Punit Singh Koura, Anjali Sridhar, Tianlu Wang, and Luke Zettlemoyer. OPT: Open pre-trained transformer language models, 2022.

A SAMPLING WITHOUT REPLACEMENT WITH PRIORITY SAMPLING

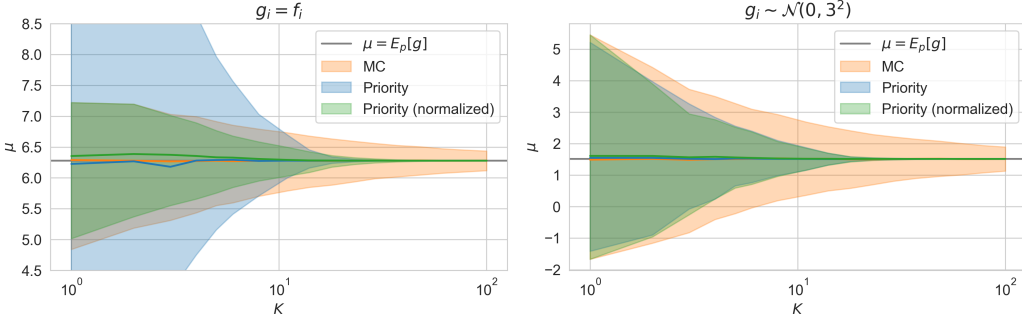


Figure 3: Estimation of $\mu = \mathbb{E}_p[g]$ with $p_i := \sum_{i=1}^N \exp f_i / \sum_{j=1}^N \exp f_j$, with $f_i \sim \mathcal{N}(0, 3^2)$ and with $N = 100$. We apply standard Monte-Carlo, priority sampling and priority sampling with self-normalized weights. We use $g_i = f_i$ in the left side of the plot, and values $g_i \sim \mathcal{N}(0, 3^2)$ sampled independently of f_i in the right side. We report the 80% CI interval given 10000 estimates, each with $K = 1 \dots 100$.

Given a set of probabilities p_1, \dots, p_N and a function with values f_1, \dots, f_N , priority sampling Duffield et al. (2007) allows estimating the sum $\sum_{i=1}^N p_i f_i$ using a subset of $K < N$ samples. For a sequence of random weights $u_1, \dots, u_n \stackrel{\text{iid}}{\sim} \text{Uniform}(0, 1]$, we define the priority keys p_i/u_i , set τ to be the $K + 1$ -th largest key, and define the set of K samples $\mathbb{S} = \{i \in [1, N] \mid p_i/u_i > \tau\}$. Using importance-weights $s_i := \max(p_i, \tau)$, priority sampling is an unbiased estimate as:

$$\mathbb{E}_{p(u_1, \dots, u_N)} \left[\sum_{i \in \mathbb{S}} s_i f_i \right] = \sum_{i=1}^N p_i f_i. \quad (17)$$

We recommend Vieira (2017) for a great introduction to priority sampling.

Self-normalized importance sampling Empirically, the estimator 17 might suffer from high variance. We follow Kool et al. (2019a) and use self-normalize importance weights defined as $\tilde{s}_i := s_i / \sum_{j \in \mathbb{S}} s_j$ to reduce variance at the cost of introducing a bias. However, the estimator $\sum_{i \in \mathbb{S}} \tilde{s}_i f_i$ is biased but consistent: it equals the true expected value for $K = N$. In Figure 3, we visualize the variance of a standard Monte-Carlo (MC) estimator in two cases, a priority sampling estimator and a priority sampling estimator with self-normalized weights. In both cases, the variance of the self-normalized priority estimate is upper-bounded by the variance of the standard MC estimate and converges to zero at a faster rate than the traditional MC estimator. In one of the two cases, the un-normalized priority estimator suffers from large variance.

B ESTIMATION OF THE RVB USING IMPORTANCE SAMPLING

We first summarize the properties of the RVB, notably by documenting its relation with the standard importance-weighted bound. As a second step, we derive the RVB estimates along with their properties.

B.1 PROPERTIES OF THE RVB ESTIMATE

Relation to the standard importance-weighted bound Without priority sampling, without the approximation of the normalizing constants, and using a set $\mathbf{d}_1, \dots, \mathbf{d}_K \sim r_\phi(\mathbf{d} \mid \mathbf{a}, \mathbf{q})$ sampled with replacement, the original importance-weighted estimate

$$L_\alpha^K(\mathbf{d}, \mathbf{q}) := \frac{1}{1 - \alpha} \log \sum_{j=1}^K w_{\theta, \phi}^{1-\alpha}(\mathbf{a}, \mathbf{d}_j, \mathbf{q}) \quad (18)$$

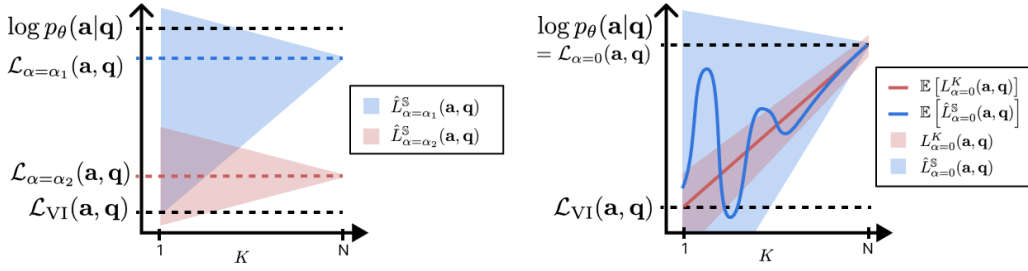


Figure 4: Log-likelihood, ELBO and RVB estimates for $K = |\mathbb{S}|$ samples. **(Left)** RVB for $0 < \alpha_1 < \alpha_2 < 1$ and the corresponding range of values for the importance-weighted estimate $\hat{L}_{\alpha=\alpha_1}^S(\mathbf{a}, \mathbf{q})$ and its estimate $\hat{L}_{\alpha=\alpha_2}^S(\mathbf{a}, \mathbf{q})$. **(Right)** Approximation of the log-likelihood using two RVB estimates: $L_{\alpha=0}^K$ the standard importance-weighted bound (Burda et al., 2015), and our tractable estimation $\hat{L}_{\alpha=0}^S$. We schematize the range of values for the estimates and their expected values.

of the RVB is a lower-bound of the log-likelihood and for $\alpha = 0$, increasing the number of samples results in a tighter log-likelihood bound (Burda et al., 2015):

$$\log p_\theta(\mathbf{a}, \mathbf{q}) \geq L_{\alpha=0}^{K+1}(\mathbf{d}, \mathbf{q}) \geq L_{\alpha=0}^K \geq \mathcal{L}_{\text{VI}}(\mathbf{a}, \mathbf{q}) . \quad (19)$$

However, the RVB estimate \hat{L}_{α}^S is only an approximation of the original importance-weighted bound.

Consistent estimation of the importance-weighted bound Our approximation to the importance-weighted bound is biased because it involves two approximations:

1. we use priority sampling, which is unbiased but using self-normalized priority sampling is biased but consistent (see section A)
2. we approximate $w_{\theta, \phi}(\mathbf{a}, \mathbf{d}, \mathbf{q})$ with a biased self-normalizing estimate, which is biased but also consistent (see section B.2.1)

Because of this loss of unbiasedness, and in contrast to the standard importance-weighted bound, the RVB estimate \hat{L}_{α}^S is not guaranteed to be a log-likelihood lower bound. Nonetheless, the RVB, the gradient and the retriever log-density gradient are all consistent: they converge to their respective expected value in the limit $K = N$ (see sections B.2.1 and B.2.2).

In figure 4, we schematize the relationship between the log-likelihood, the RVB, and the range of importance sampling estimates. Even though we cannot guarantee the unbiasedness of the estimate, self-normalized estimates (such as ours) are widely used in the literature. We refer the reader to Elvira & Martino (2021) for an updated review of importance sampling.

Complexity $\mathcal{O}(K)$ All estimates require one backbone (i.e., BERT) call to encode the query and one call to encode each of the K sampled documents. Neglecting the other operations required to evaluate the RVB, this results in a computational complexity of $\mathcal{O}(1 + K) \approx \mathcal{O}(K)$.

B.2 RATIO OF NORMALIZING CONSTANTS

The ratio of un-normalized retriever densities $\zeta(\mathbf{d}) := \exp f_\theta(\mathbf{d}, \mathbf{q}) / \exp f_\phi(\mathbf{a}, \mathbf{d}, \mathbf{q})$ can be used to express the ratio of normalizing constants with the following equality:

$$\frac{\sum_{\mathbf{d} \in \mathbb{T}_\phi} \exp f_\theta(\mathbf{d}, \mathbf{q})}{\sum_{\mathbf{d}' \in \mathbb{T}_\phi} \exp f_\phi(\mathbf{a}, \mathbf{d}', \mathbf{q})} = \mathbb{E}_{r_\phi(\mathbf{d}|\mathbf{a}, \mathbf{q})} [\zeta(\mathbf{d})] . \quad (20)$$

We use the above equality to estimate $w_{\theta,\phi}(\mathbf{a}, \mathbf{d}, \mathbf{q})$ and $\nabla_{\theta} \log p_{\theta}(\mathbf{d} \mid \mathbf{q})$ during training and evaluation. The equality arises from the definition of the right-hand term:

$$\mathbb{E}_{r_{\phi}(\mathbf{d} \mid \mathbf{a}, \mathbf{q})} [\zeta(\mathbf{d})] := \sum_{\mathbf{d} \in \mathbb{T}_{\phi}} r_{\phi}(\mathbf{d} \mid \mathbf{a}, \mathbf{q}) \frac{\exp f_{\theta}(\mathbf{d}, \mathbf{q})}{\exp f_{\phi}(\mathbf{a}, \mathbf{d}, \mathbf{q})} \quad (21)$$

$$= \sum_{\mathbf{d} \in \mathbb{T}_{\phi}} \frac{\exp f_{\phi}(\mathbf{a}, \mathbf{d}, \mathbf{q})}{\sum_{\mathbf{d}' \in \mathbb{T}_{\phi}} \exp f_{\phi}(\mathbf{a}, \mathbf{d}', \mathbf{q})} \frac{\exp f_{\theta}(\mathbf{d}, \mathbf{q})}{\exp f_{\phi}(\mathbf{a}, \mathbf{d}, \mathbf{q})}. \quad (22)$$

B.2.1 RVB ESTIMATE

We apply self-normalized priority sampling (see Appendix A) to estimate $\mathbb{E}_{r_{\phi}(\mathbf{d} \mid \mathbf{a}, \mathbf{q})} [w_{\theta,\phi}^{1-\alpha}(\mathbf{a}, \mathbf{d}, \mathbf{q})]$.

We denote $\mathbb{S} = \{\mathbf{d}_1, \dots, \mathbf{d}_K\}$ the set of documents sampled without replacement and $\tilde{s}(\mathbf{d}_1), \dots, \tilde{s}(\mathbf{d}_K)$ the self-normalized priority importance weights. This gives an estimate of the RVB that is consistent (i.e., it converges to the true value in the limit $K = N$ with probability 1):

$$\mathcal{L}_{\alpha}(\mathbf{a}, \mathbf{q}) := \frac{1}{1-\alpha} \log \mathbb{E}_{r_{\phi}(\mathbf{d} \mid \mathbf{a}, \mathbf{q})} [w_{\theta,\phi}^{1-\alpha}(\mathbf{a}, \mathbf{d}, \mathbf{q})] \quad (23)$$

$$\approx \frac{1}{1-\alpha} \log \sum_{\mathbf{d} \in \mathbb{S}} \tilde{s}(\mathbf{d}) w_{\theta,\phi}^{1-\alpha}(\mathbf{a}, \mathbf{d}, \mathbf{q}) := \hat{L}_{\alpha}^{\mathbb{S}}(\mathbf{a}, \mathbf{q}). \quad (24)$$

Evaluating the weights $w_{\theta,\phi}(\mathbf{a}, \mathbf{d}, \mathbf{q})$ requires estimating the normalizing constant of $p_{\theta}(\mathbf{d} \mid \mathbf{q})$, which would require P backbone (e.g. BERT) calls. Using the identity 20, we obtain a self-normalized estimate of the weight:

$$w_{\theta,\phi}(\mathbf{a}, \mathbf{d}, \mathbf{q}) := \frac{p_{\theta}(\mathbf{a} \mid \mathbf{d}, \mathbf{q}) p_{\theta}(\mathbf{d} \mid \mathbf{q})}{r_{\phi}(\mathbf{d} \mid \mathbf{a}, \mathbf{q})} \quad (25)$$

$$= p_{\theta}(\mathbf{a} \mid \mathbf{d}, \mathbf{q}) \zeta(\mathbf{d}) \left(\frac{\sum_{\mathbf{d}' \in \mathbb{T}_{\phi}} \exp f_{\theta}(\mathbf{d}', \mathbf{q})}{\sum_{\mathbf{d}' \in \mathbb{T}_{\phi}} \exp f_{\phi}(\mathbf{a}, \mathbf{d}, \mathbf{q}')} \right)^{-1} \quad (26)$$

$$= p_{\theta}(\mathbf{a} \mid \mathbf{d}, \mathbf{q}) \zeta(\mathbf{d}) (\mathbb{E}_{r_{\phi}(\mathbf{d} \mid \mathbf{a}, \mathbf{q})} [\zeta(\mathbf{d})])^{-1} \quad (27)$$

$$\approx \frac{p_{\theta}(\mathbf{a} \mid \mathbf{d}, \mathbf{q}) \zeta(\mathbf{d})}{\sum_{\mathbf{d}' \in \mathbb{T}_{\phi}} \tilde{s}(\mathbf{d}') \zeta(\mathbf{d}')}. \quad (28)$$

This estimate requires only $K \leq P$ backbone calls and is consistent because the denominator $\mathbb{E}_{r_{\phi}(\mathbf{d} \mid \mathbf{a}, \mathbf{q})} [\zeta(\mathbf{d})]$ is estimated using a consistent self-normalized priority sampling estimator. Finally, by combining the two previous steps, we obtain the estimate of the RVB defined in Equation 10. The resulting RVB estimate is consistent because it combines consistent estimators.

B.2.2 RVB GRADIENT ESTIMATE

Using the results from the previous section, the gradient of the RVB w.r.t the parameter θ can be estimated as:

$$\nabla_{\theta} \mathcal{L}_{\alpha}(\mathbf{a}, \mathbf{q}) := \mathbb{E}_{r_{\phi}(\mathbf{d} \mid \mathbf{a}, \mathbf{q})} \left[\widetilde{w}_{\theta,\phi}^{1-\alpha}(\mathbf{a}, \mathbf{d}, \mathbf{q}) \nabla_{\theta} \log p_{\theta}(\mathbf{a}, \mathbf{d} \mid \mathbf{q}) \right] \quad (29)$$

$$:= \mathbb{E}_{r_{\phi}(\mathbf{d} \mid \mathbf{a}, \mathbf{q})} \left[\frac{w_{\theta,\phi}^{1-\alpha}(\mathbf{a}, \mathbf{d}, \mathbf{q})}{\mathbb{E}_{r_{\phi}(\mathbf{d}' \mid \mathbf{a}, \mathbf{q})} [w_{\theta,\phi}^{1-\alpha}(\mathbf{a}, \mathbf{d}', \mathbf{q})]} \nabla_{\theta} \log p_{\theta}(\mathbf{a}, \mathbf{d} \mid \mathbf{q}) \right] \quad (30)$$

$$\approx \mathbb{E}_{r_{\phi}(\mathbf{d} \mid \mathbf{a}, \mathbf{q})} \left[\frac{\left(p_{\theta}(\mathbf{a} \mid \mathbf{d}, \mathbf{q}) \zeta(\mathbf{d}) / \sum_{\mathbf{d}'' \in \mathbb{T}_{\phi}} \tilde{s}(\mathbf{d}'') \zeta(\mathbf{d}'') \right)^{1-\alpha}}{\mathbb{E}_{r_{\phi}(\mathbf{d}' \mid \mathbf{a}, \mathbf{q})} \left[\left(p_{\theta}(\mathbf{a} \mid \mathbf{d}', \mathbf{q}) \zeta(\mathbf{d}') / \sum_{\mathbf{d}''' \in \mathbb{T}_{\phi}} \tilde{s}(\mathbf{d}''') \zeta(\mathbf{d}''') \right)^{1-\alpha} \right]} \nabla_{\theta} \log p_{\theta}(\mathbf{a}, \mathbf{d} \mid \mathbf{q}) \right] \quad (31)$$

$$\approx \sum_{\mathbf{d} \in \mathbb{S}} \frac{\tilde{s}(\mathbf{d}) (p_{\theta}(\mathbf{a} \mid \mathbf{d}, \mathbf{q}) \zeta(\mathbf{d}))^{1-\alpha}}{\sum_{\mathbf{d}' \in \mathbb{S}} \tilde{s}(\mathbf{d}') (p_{\theta}(\mathbf{a} \mid \mathbf{d}', \mathbf{q}) \zeta(\mathbf{d}'))^{1-\alpha}} \nabla_{\theta} \log p_{\theta}(\mathbf{a}, \mathbf{d} \mid \mathbf{q}). \quad (32)$$

Another approximation is required to estimate $\log p_\theta(\mathbf{a}, \mathbf{d} \mid \mathbf{q}) = \log p_\theta(\mathbf{q} \mid \mathbf{d}, \mathbf{q}) + \log p_\theta(\mathbf{d} \mid \mathbf{q})$ without evaluating $\sum_{\mathbf{d} \in \mathbb{T}_\phi} \exp f_\theta(\mathbf{d}, \mathbf{q})$. This approximation is also consistent because self-normalized priority sampling is consistent:

$$\nabla_\theta \log p_\theta(\mathbf{d} \mid \mathbf{q}) = \nabla_\theta f_\theta(\mathbf{d}, \mathbf{q}) - \nabla_\theta \log \sum_{\mathbf{d}' \in \mathbb{T}_\phi} \exp f_\theta(\mathbf{d}', \mathbf{q}) \quad (33)$$

$$= \nabla_\theta f_\theta(\mathbf{d}, \mathbf{q}) - \frac{\nabla_\theta \sum_{\mathbf{d}' \in \mathbb{T}_\phi} \exp f_\theta(\mathbf{d}', \mathbf{q})}{\sum_{\mathbf{d}'' \in \mathbb{T}_\phi} \exp f_\theta(\mathbf{d}'', \mathbf{q})} \quad (34)$$

$$= \nabla_\theta f_\theta(\mathbf{d}, \mathbf{q}) - \sum_{\mathbf{d}' \in \mathbb{T}_\phi} p_\theta(\mathbf{d}' \mid \mathbf{q}) \nabla_\theta f_\theta(\mathbf{d}', \mathbf{q}) \quad (35)$$

$$= \nabla_\theta f_\theta(\mathbf{d}, \mathbf{q}) - \sum_{\mathbf{d}' \in \mathbb{T}_\phi} r_\phi(\mathbf{d}' \mid \mathbf{a}, \mathbf{q}) \frac{p_\theta(\mathbf{d}' \mid \mathbf{q})}{r_\phi(\mathbf{d}' \mid \mathbf{a}, \mathbf{q})} \nabla_\theta f_\theta(\mathbf{d}', \mathbf{q}) \quad (36)$$

$$= \nabla_\theta f_\theta(\mathbf{d}, \mathbf{q}) - \sum_{\mathbf{d}' \in \mathbb{T}_\phi} r_\phi(\mathbf{d}' \mid \mathbf{a}, \mathbf{q}) \frac{\zeta(\mathbf{d}')}{\mathbb{E}_{r_\phi(\mathbf{d}' \mid \mathbf{a}, \mathbf{q})} [\zeta(\mathbf{d}'')]} \nabla_\theta f_\theta(\mathbf{d}', \mathbf{q}) \quad (37)$$

$$\approx \nabla_\theta f_\theta(\mathbf{d}, \mathbf{q}) - \sum_{\mathbf{d}' \in \mathbb{T}_\phi} \frac{\tilde{s}(\mathbf{d}') \zeta(\mathbf{d}')}{\sum_{\mathbf{d}'' \in \mathbb{T}_\phi} \tilde{s}(\mathbf{d}'') \zeta(\mathbf{d}'')} \nabla_\theta f_\theta(\mathbf{d}', \mathbf{q}) . \quad (38)$$

C APPLICATIONS OF THE VOD FRAMEWORK

In this section, we detail how to apply the VOD framework to the tasks of language modelling as well as extractive, generative and multiple-choice ODQA. We also detail a solution to optimizing multi-documents readers (FiD) jointly.

C.1 GENERATIVE AND EXTRACTIVE ODQA

The model $p_\theta(\mathbf{a} \mid \mathbf{d}, \mathbf{q})$ a machine reading comprehension component that can be implemented either using an extractive approach, as done in the original BERT (Devlin et al., 2018), or using a generative approach Lewis et al. (2019). Applying the VOD framework to generative and extractive ODQA simply requires plugging the likelihood of the corresponding machine reading comprehension model $p_\theta(\mathbf{a} \mid \mathbf{d}, \mathbf{q})$ in the RVB and gradient estimates (equations 10 and 11).

C.2 RETRIEVAL-AUGMENTED LANGUAGE MODELLING

We consider the variable $\mathbf{a} = [\mathbf{a}_1, \dots, \mathbf{a}_T]$ to be the sequence of tokens of length T and omit the condition \mathbf{q} . We consider a left-to-right factorization $p_\theta(\mathbf{a}) := \prod_{t=1}^T p_\theta(\mathbf{a}_t \mid \mathbf{a}_{<t})$ and define the following retrieval-augmented language model with one retrieved document per token:

$$p_\theta(\mathbf{a}) := \prod_{t=1}^T \sum_{\mathbf{d}_t \in \mathbb{D}} p_\theta(\mathbf{d}_t \mid \mathbf{a}_{<t}) p_\theta(\mathbf{a}_t \mid \mathbf{d}_t, \mathbf{a}_{<t}) . \quad (39)$$

We apply the RVB to each step t using an approximate posterior $r_\phi(\mathbf{d}_t \mid \mathbf{a})$, this results in the following log-likelihood lower bound for $\alpha \geq 0$:

$$\log p_\theta(\mathbf{a}) \geq \log \prod_{t=1}^T \mathcal{L}_\alpha(\mathbf{a}_t, \mathbf{a}_{<t}) \quad (40)$$

$$= \frac{1}{1-\alpha} \sum_{t=1}^T \log \mathbb{E}_{r_\phi(\mathbf{d} \mid \mathbf{a}, \mathbf{q})} \left[w_{\theta, \phi}^{1-\alpha}(\mathbf{a}_t, \mathbf{d}_t, \mathbf{a}_{<t}) \right] . \quad (41)$$

The above step-wise RVB $\mathcal{L}_\alpha(\mathbf{a}_t, \mathbf{a}_{<t})$ can be estimated using equations 10 and 11.

C.3 MULTIPLE-CHOICE ODQA

In the multiple-choice setting, a vector of M answer options $\mathbf{A} := [\mathbf{a}_1, \dots, \mathbf{a}_M]$ is given. We denote \mathbf{a} the correct option and assume $\mathbf{a} \in \mathbf{A}$. We define the vector of M queries as $\mathbf{Q} = [\mathbf{q}_1, \dots, \mathbf{q}_M]$ with $\mathbf{q}_j := [\mathbf{q}; \mathbf{a}_j]$ where $[\cdot; \cdot]$ denotes the concatenation operator. We denote \times the Cartesian product, $\mathbf{D} = [\mathbf{d}_1, \dots, \mathbf{d}_M]$ a vector of M documents, and $\mathbb{D}^{(M)} := \mathbb{D} \times \dots \times \mathbb{D}$ the set of combinations of vectors of M documents (N^M document vectors). We choose:

$$p_\theta(\mathbf{a}_* | \mathbf{D}, \mathbf{Q}) := \frac{\exp g_\theta(\mathbf{d}_*, \mathbf{q}_*)}{\sum_{j=1}^M \exp g_\theta(\mathbf{d}_j, \mathbf{q}_j)} \quad (42)$$

$$p_\theta(\mathbf{D} | \mathbf{Q}) := \prod_{j=1}^M p_\theta(\mathbf{d}_j | \mathbf{q}_j) \quad (43)$$

$$r_\phi(\mathbf{D} | \mathbf{A}, \mathbf{Q}) := \prod_{j=1}^M r_\phi(\mathbf{d}_j | \mathbf{q}_j). \quad (44)$$

Given a set of K documents \mathbb{S}_j sampled without replacement from $r_\phi(\mathbf{d}_j | \mathbf{q}_j)$ for each option j and with priority weights $s_j(\mathbf{d}_j)$, we denote $\mathbb{S}^{(M)} := \mathbb{S}_1 \times \dots \times \mathbb{S}_M$ the Cartesian product of the sets of per-option samples. Because the components of \mathbf{D} are independent (equation 44), priority sampling can be applied to the product $r_\phi(\mathbf{D} | \mathbf{Q})$ with self-normalized weights $\tilde{s}(\mathbf{D}) := \prod_{j=1}^M s_j(\mathbf{d}_j)$. For an arbitrary function $h(\mathbf{D})$, we have:

$$\begin{aligned} \mathbb{E}_{r_\phi(\mathbf{D} | \mathbf{Q})} [h(\mathbf{D})] &= \mathbb{E}_{r_\phi(\mathbf{d}_1 | \mathbf{q}_1)} [\dots \mathbb{E}_{r_\phi(\mathbf{d}_M | \mathbf{q}_M)} [h(\mathbf{D})] \dots] \\ &\approx \sum_{\mathbf{d}_1 \in \mathbb{D}} \tilde{s}(\mathbf{d}_1) \dots \sum_{\mathbf{d}_M \in \mathbb{D}} \tilde{s}(\mathbf{d}_M) h(\mathbf{D}) \\ &= \sum_{\mathbf{D} \in \mathbb{S}^{(M)}} \tilde{s}(\mathbf{D}) h(\mathbf{D}). \end{aligned}$$

We have defined a model for multiple-choice and showed that priority sampling can be applied to the product $r_\phi(\mathbf{D} | \mathbf{Q})$ with weights $\tilde{s}(\mathbf{D}) := \prod_{j=1}^M s_j(\mathbf{d}_j)$, we will now show how the RVB estimates can be adapted to the multiple-choice setting. The derivation is identical to the one presented in section B. This arises from the fact that there are functions $F_\theta(\mathbf{D}, \mathbf{Q}) := \sum_{j=1}^M f_\theta(\mathbf{d}_j, \mathbf{q}_j)$ and $F_\phi(\mathbf{A}, \mathbf{D}, \mathbf{Q}) := \sum_{j=1}^M f_\phi(\mathbf{d}_j, \mathbf{q}_j)$ and a set $\mathcal{T}_\phi := \{\mathbf{D} \in \mathbb{D}^{(M)} | \forall j \in [1, M], \mathbf{d} \in \mathbb{T}_\phi(\mathbf{q}_j)\}$, the ensemble of the top- P documents for each query \mathbf{q}_j , such that

$$p_\theta(\mathbf{D} | \mathbf{Q}) \propto \mathbb{1}[\mathbf{D} \in \mathcal{T}_\phi] \exp F_\theta(\mathbf{D}, \mathbf{Q}) \quad (45)$$

$$r_\phi(\mathbf{D} | \mathbf{A}, \mathbf{Q}) \propto \mathbb{1}[\mathbf{D} \in \mathcal{T}_\phi] \exp F_\phi(\mathbf{A}, \mathbf{D}, \mathbf{Q}). \quad (46)$$

By applying the results from section B to $\mathbf{A}, \mathbf{D}, \mathbf{Q}$ with $\zeta(\mathbf{D}) = \exp F_\theta(\mathbf{D}, \mathbf{Q}) / \exp F_\phi(\mathbf{A}, \mathbf{D}, \mathbf{Q})$ the RVB and its gradients can be estimated using:

$$\mathcal{L}_\alpha(\mathbf{a}_*, \mathbf{Q}) \approx \hat{L}_\alpha^{\mathbb{S}^{(M)}}(\mathbf{a}_*, \mathbf{Q}) := \frac{1}{1-\alpha} \log \sum_{\mathbf{D} \in \mathbb{S}^{(M)}} \tilde{s}(\mathbf{D}) \left(\frac{\zeta(\mathbf{D}) p_\theta(\mathbf{A} | \mathbf{D}, \mathbf{Q})}{\sum_{\mathbf{D}' \in \mathbb{S}^{(M)}} \tilde{s}(\mathbf{D}') \zeta(\mathbf{D}')} \right)^{1-\alpha} \quad (47)$$

$$\nabla_\theta \mathcal{L}_\alpha(\mathbf{A}, \mathbf{Q}) \approx \sum_{\mathbf{D} \in \mathbb{S}^{(M)}} \frac{\tilde{s}(\mathbf{D}) (\zeta(\mathbf{D}) p_\theta(\mathbf{A} | \mathbf{D}, \mathbf{Q}))^{1-\alpha}}{\sum_{\mathbf{D}' \in \mathbb{S}^{(M)}} \tilde{s}(\mathbf{D}') (\zeta(\mathbf{D}') p_\theta(\mathbf{A} | \mathbf{D}', \mathbf{Q}))^{1-\alpha}} \nabla_\theta \log p_\theta(\mathbf{A}, \mathbf{D} | \mathbf{Q}). \quad (48)$$

Monte-Carlo estimation During training, the computational budget is tight, and the RVB and its gradient are estimated using a single set of samples $\mathbb{S}^{(M)}$. During evaluation, we can leverage $C \geq 1$ Monte-Carlo samples $\mathbb{S}_1^M, \dots, \mathbb{S}_C^M$, each containing K^M documents sampled from $r_\phi(\mathbf{D} | \mathbf{A}, \mathbf{Q})$ without replacement, to estimate the RVB (and therefore the log-likelihood) more accurately. We use the following estimate:

$$\hat{p}_\theta(\mathbf{a}, \mathbf{Q}) := \frac{1}{C} \sum_{i=1}^C \frac{\exp \hat{L}_\alpha^{\mathbb{S}_i^{(M)}}(\mathbf{a}, \mathbf{q})}{\sum_{\mathbf{a}' \in \mathbf{A}} \exp \hat{L}_\alpha^{\mathbb{S}_i^{(M)}}(\mathbf{a}', \mathbf{Q})}. \quad (49)$$

C.4 FUSION-IN-DECODER (FiD)

In this work, we considered reader models $p_\theta(\mathbf{a}|\mathbf{d}, \mathbf{q})$ with a single document per sample. Alternatively, models such as FiD (Izacard & Grave, 2020b) implement a reader model that allows reading multiple documents per sample. Given a set $\mathbb{S} := \{\mathbf{d}_1, \dots, \mathbf{d}_K\}$ of documents, we denote the multi-document reader $p_\theta(\mathbf{a}|\mathbb{S}, \mathbf{q})$. Defining a distribution over the set of unique documents $p(\mathbb{S})$ with tractable sampling and density evaluation is challenging. EMDR² (Sachan et al., 2021b) optimized a multi-document reader jointly with a deep retriever. However, an auxiliary reader model $p_\theta(\mathbf{a}|\mathbb{S}, \mathbf{q}) := \prod_{i=1}^K p_\theta(\mathbf{a}|\mathbf{d}_i, \mathbf{q})$ is used to optimize a retriever model $p_\theta(\mathbb{S}|\mathbf{q}) := \prod_{i=1}^K p_\theta(\mathbf{d}_i|\mathbf{q})$. VOD can be applied by following the same strategy, and this is equivalent to optimizing a single-sample joint reader along with a multi-sample reader:

$$L_{\text{MULTISAMPLE}} := \underbrace{\nabla_\theta \log p_\theta(\mathbf{a}|\mathbb{S}, \mathbf{q})}_{\text{multi-sample reader likelihood}} + \underbrace{\sum_{\mathbf{d} \in \mathbb{S}} \tilde{s}(\mathbf{d}) \tilde{w}_{\theta, \phi}^{1-\alpha}(\mathbf{a}, \mathbf{d}|\mathbb{S}) \nabla_\theta \log p_\theta(\mathbf{a}, \mathbf{d}|\mathbf{q})}_{\text{single-sample RVB gradient}}. \quad (50)$$

D EXPERIMENTAL RESULTS

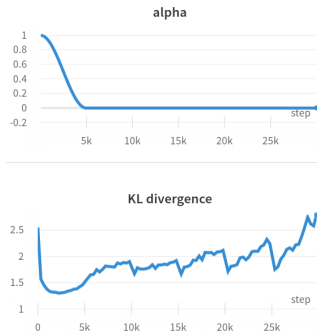


Figure 5: Measure of the divergence $D_{\text{KL}}(r_\phi(\mathbf{d}|\mathbf{q}) \parallel p_\theta(\mathbf{d}|\mathbf{q}))$ during the training of a VOD retriever on the USMLE dataset. The retriever checkpoint is updated every $T = 5k$ steps. α is annealed from 1 to 0 during the first 5k steps. We recognize the pattern schematized in Figure 1. In this example, the approximate posterior is chosen as a combination of a checkpoint of the retriever and a static BM25 component. Therefore the value of the divergence is never zero because the divergence between the model and the BM25 retriever is always strictly positive.

E IMPLEMENTATION

Table 8: Parameterization of the reader and retriever scores. The complexity is reported for a batch-size of one, M answer option, and for K documents and inputs $\mathbf{q}_j = [\mathbf{q}; \mathbf{a}_j]$ and \mathbf{d} of lengths $L_{\mathbf{q}}$ and $L_{\mathbf{a}}$. When using a dual-encoder architecture, the parameters are shared across the two encoders.

Type	Complexity	Parameterization
dual-encoder	$M(L_{\mathbf{q}}^2 + KL_{\mathbf{d}}^2)$	$f_\theta(\mathbf{d}, \mathbf{q}_j) = \text{Linear}_{\theta D}(\text{BERT}_\theta(\mathbf{d}))^T \text{Linear}_{\theta Q}(\text{BERT}_\theta(\mathbf{q}_j))$
Cross attn.	$MK(L_{\mathbf{q}} + L_{\mathbf{d}})^2$	$g_\theta(\mathbf{d}, \mathbf{q}_j) = \text{Linear}_\theta(\text{BERT}_\theta([\mathbf{d}; \mathbf{q}_j]))$

Documents preprocessing We encode the text and title of all the articles using the relevant BERT tokenizer. For each article with encoded title \mathbf{t} of length $L_{\mathbf{t}}$, we extract overlapping passages \mathbf{p} of length $200 - 1 - t$ with stride 100 tokens. For each passage, using [DOC] a special token added to the BERT vocabulary, we format each passage as

$$\mathbf{d} := [\text{CLS}] ; [\text{DOC}] ; \mathbf{t} ; \mathbf{p}. \quad (51)$$

Queries preprocessing We encode all questions and answer options using the tokenizer and store the question-answer pairs as

$$\mathbf{q}_j := [\text{CLS}] ; [\text{QUERY}] ; \mathbf{q} ; [\text{SEP}] ; \mathbf{a}_j \quad (52)$$

where the question \mathbf{q} is truncated such as $|\mathbf{q}_j| \leq 312$ tokens and [QUERY] is an additional special token. On the reader side, we append the document passage \mathbf{d} to the question-answer query q_j such that $\mathbf{q}_j := [\mathbf{d}; [\text{SEP}]; [\text{QUERY}]; \mathbf{q}; [\text{SEP}]; \mathbf{a}_j]$.

Reader We parameterize the reader score g_θ using a cross-attention model parameterized by another BERT backbone. Each query $\mathbf{q}_j = [\mathbf{q}; \mathbf{a}_j]$ is prepended with a document \mathbf{d} , and an additional linear layer is used to reduce the output of BERT at the `CLS` token to a scalar value, as originally done in Devlin et al. (2018). See expression in Table 8.

Retriever We parameterize the retriever score f_θ using a dual encoder architecture similar to DPR, except that we share the BERT backbone across the two columns and one linear layer to project the output of each column. See expression in Table 8.

Hyperparameters We summarize the training, evaluation and model hyperparameters in Table 9.

Table 9: Hyperparameters used across the multiple-choice ODQA experiments.

Category	Parameter	Value
Optimization	Optimizer	AdamW
	Learning rate	$3 \cdot 10^{-6}$
	Learning rate warmup	$0.1 \cdot T$
	Warmup frequency	every T steps
	Weight decay	$1 \cdot 10^{-3}$
	Gradient clipping	0.5
	Precision	<code>float16</code>
α annealing	initial value	1
	final value	0
	length	T steps
	type	cosine
Model	Reader	BioLinkBERT + linear layer
	Retriever	BioLinkBERT + two linear layers
	Output vector size	768
Batching	batch-size	32
	M (# of options)	4
	K (documents per option)	8
	P (retriever support size)	100
	N (corpus size)	7,766.9k
	document passage stride	100
	L_d (document passage length)	200
	max. L_q (max. query length)	312
	max. $L_d + L_q$	512
Training	T (re-indexing period length)	5k
	Training steps (MedMCQA)	150k
	Training steps (USMLE)	50k
	Training steps (MedMCQA \rightarrow USMLE)	150k \rightarrow 10k
	Training steps (MedMCQA + USMLE)	–
	Training steps (Distillation)	120k
Posterior and retrieval	parameterization	$f_\phi^{\text{ckpt}}(\mathbf{d}, [\mathbf{q}; \mathbf{a}]) + \tau^{-1}(\text{BM25}(\mathbf{q}) + \beta \cdot \text{BM25}(\mathbf{a}))$
	τ (BM25 temperature)	5
	β (BM25 answer weight)	$1 + 0.5 \max\{0, \log(L_q/L_a)\}$
	BM25 implementation	elasticsearch v7.14.1
	BM25 parameters	$b=0.75, k1=1.2$
	MIPS implementation	faiss v1.7.2
	faiss factory string	IVF1000,Flat
	faiss precision	<code>float16</code>
	faiss nprobe	32
Evaluation	C (Monte-Carlo samples for eval.)	10
Hardware	CPU	AMD EPYC 7252 8-Core Processor
	RAM	256 GB
	GPU	8 \times Quadro RTX 5000
	VRAM	128 GB
Software	PyTorch	Paszke et al. (2019)
	Lightning	Falcon
	faiss	Johnson et al. (2021)

F SYMBOLS

Table 10: Mathematical symbols.

Category	Symbol	Description
ODQA variables	\mathbf{a}	answer
	\mathbf{d}	document or document passage
	\mathbf{q}	question or query
	L_a	number of tokens in the answer
	L_d	number of tokens in the document
	L_q	number of tokens in the query
	\mathbb{D}	corpus of documents
Reader-retriever	N	number of documents in the corpus
	θ	parameter of the retrieval-augmented model (generative model)
	$p_\theta(\mathbf{a}, \mathbf{d} \mathbf{q})$	Joint reader-retriever model
	$w_{\theta, \phi}(\mathbf{a}, \mathbf{d}, \mathbf{q})$	Importance weight
	$\zeta(\mathbf{d})$	ratio of exponentiated scores $\exp f_\theta(\mathbf{d}, \mathbf{q})/\exp f_\phi(\mathbf{a}, \mathbf{d}, \mathbf{q})$
	$p_\theta(\mathbf{a} \mathbf{d}, \mathbf{q})$	reader
	$p_\theta(\mathbf{d} \mathbf{q})$	retriever
Posterior	$f_\theta(\mathbf{d}, \mathbf{q})$	score of the retriever
	ϕ	parameter of the approximate posterior (inference network)
	$r_\phi(\mathbf{d} \mathbf{a}, \mathbf{q})$	approximate posterior (static retriever)
	$f_\phi(\mathbf{a}, \mathbf{d}, \mathbf{q})$	score of the approximate posterior
	$\text{BM25}(\mathbf{q}, \mathbf{d})$	BM25 score of the query \mathbf{q} for the document \mathbf{d}
	$f_\phi^{\text{ckpt}}(\mathbf{d}, \mathbf{q})$	checkpoint of the retriever f_θ at step $k \cdot T$
	τ	temperature balancing the checkpoint score and the BM25 score
Truncated retriever	β	weight balancing the query and answer options BM25 terms
	P	number of documents with non-zero mass under $p_\theta(\mathbf{d} \mathbf{q})$
	\mathbb{T}_ϕ	set of top- P documents ranked by f_ϕ
Sampling	\mathbb{S}	set of K documents sampled without replacement from $r_\phi(\mathbf{d} \mathbf{a}, \mathbf{q})$
	$s(\mathbf{d})$	value of the priority weight for the document \mathbf{d} , $s(\mathbf{d}) = 0$ if $\mathbf{d} \notin \mathbb{S}$
	K	number of document samples with $K \leq P \leq N$
	C	number of Monte-Carlo samples (evaluation)
Bounds	$\log p_\theta(\mathbf{a}, \mathbf{q})$	Marginal task likelihood
	$\mathcal{L}_{\text{VI}}(\mathbf{a}, \mathbf{q})$	Variational Lower bound (ELBO)
	$\mathcal{L}_\alpha(\mathbf{a}, \mathbf{q})$	Rényi Variational Bound (RVB)
	α	parameter of the RVB $\alpha \geq 0$
	$\hat{L}_\alpha^{\mathbb{S}}(\mathbf{a}, \mathbf{q})$	tractable RVB estimate given a set of \mathbb{S} samples
	$\hat{L}_\alpha^K(\mathbf{a}, \mathbf{q})$	standard RVB estimate given a set of K Monte-Carlo samples
	$D_{\text{KL}}(r_\phi(\mathbf{d} \mathbf{a}, \mathbf{q}) \parallel p_\theta(\mathbf{d} \mathbf{a}, \mathbf{q}))$	KL divergence between the true and the approximate posteriors
Multiple-choice	\mathbf{a}_i	answer option i
	$*$	index of the correct answer option
	\mathbf{q}_i	question-answer pair $[\mathbf{q}; \mathbf{a}_i]$
	M	number of answer options
	\mathbf{A}	vector of M answer choices
	\mathbf{D}	vector of M documents
	\mathbf{Q}	vector of M queries (each expressed as $[\mathbf{q}; \mathbf{a}_i]$)
	$g_\theta(\mathbf{d}, \mathbf{q})$	score of the reader (multiple-choice)
	$\mathbb{S}^{(M)}$	Cartesian product of the per-option samples $\mathbb{S}_1, \dots, \mathbb{S}_M$
Spaces and Sets	\mathcal{T}_ϕ	Product of the per-option top- P sets $\mathbb{T}_\phi(\mathbf{q}_1), \dots, \mathbb{T}_\phi(\mathbf{q}_M)$
	Ω	space of strings
	\mathbb{R}	reals
	$(0, 1]$	real numbers in the interval $[0, 1]$, 0 excluded
Operators	$:=$	defined as
	$[\cdot; \cdot]$	concatenation operator
	\times	Cartesian product
	$D_{\text{KL}}(r_\phi(p) \parallel q)$	Kullback–Leibler (KL) divergence between p and q
	$\mathbb{1}[\mathbf{x} \in \mathbb{X}]$	indicator function with value 1 if $\mathbf{x} \in \mathbb{X}$ otherwise 0
	$\text{argtop}_{\mathbf{x} \in \mathbb{X}}(f(\mathbf{x}); K)$	top-K values from the set \mathbb{X} as scored by f

G MEDWIKI

Table 11: Comparing the MedWiki with the original MedQA corpus on the USMLE dataset.

Method	Reader	Retriever	Corpus	Valid.	Test
Disjoint	BioBERT ¹	BM25	MedQA ²	37.68	39.54
Disjoint	BioBERT ¹	BM25	MedWiki	38.82	40.46
Disjoint	BioLinkBERT	BM25	MedQA ²	40.37	41.05
Disjoint	BioLinkBERT	BM25	MedWiki	42.21	42.25

¹model weights from Lee et al. (2020), ²original corpus from Jin et al. (2021)

The MedWiki corpus is a set of Wikipedia articles collected for research on medical question answering with low resources. Existing medical corpora, such as the MedQA corpus, are not adequately aligned with the ODQA task and are often measly and fragmented. At the same time, all of Wikipedia is cumbersome to use on consumer hardware. In order to reflect the true information need of medical experts, we assembled the MedWiki corpus by using real-world medical entrance exam questions. We queried the Wikipedia API using the answer options from all dataset splits of USMLE and MedMCQA and retained the top-10 articles for each answer option. This corpus includes 293.6k unique Wikipedia articles ($\approx 4.5\%$ of Wikipedia) that cover a broad range of medical topics.

MEDQA vs. MEDWIKI

Qualitative comparison When comparing knowledge corpora, there are two key questions: "how similar are they?" and "in what ways do they differ?". Using ElasticSearch, we compare the retrieved documents of MedWiki to the ones of MedQA. In Table 12, 13, 14 we present a few examples. The MedQA corpus is a selection of medical textbooks which often revolve around medical case studies, akin to the USMLE questions (see example in Table 12). In contrast, the MedWiki corpus references Wikipedia articles which are often edited to be concise, which is especially true for the abstract part of the articles, which contain the basic and usually most important information about a topic. Furthermore, each Wikipedia article comes with a title, which augments each passage with a higher-level context.

However, our approach of querying against the Wikipedia API results in many out-of-domain articles. For instance in Table 13, we display a MedWiki passage that originates from a non-medical article. Although the MedQA corpus is strictly oriented toward medical topics, it was built by extracting text from physical books using OCR software, which led to errors in the process and ultimately resulted in part of the corpus being unreadable.

Overall, both corpora provide adequate evidence to answer USMLE questions. Nevertheless, the MedWiki corpus is three times larger in vocabulary size and eight times more extensive in word count, making it more robust and diverse.

Quantitative comparison We investigated how the two corpora affect the final QA accuracy on the USMLE dataset. In contrast with the rest of the paper, we used a multi-document reader, as done in Jin et al. (2021). We used an ElasticSearch index to retrieve the set of top 3 documents $\{d_1, d_2, d_3\}$ for each pair (q, a_i) as context for each answer option. The normalized log probabilities over the four options were obtained by processing the set of concatenated tokens $[d_1; d_2; d_3; q; a_i]$ with BERT. We performed all experiments using a batch size of 16, set the learning rate to $1e-5$, and run all experiments for 30 epochs. We report the predictive accuracy averaged for three initial random seeds.

Table 11 summarizes the performance on the two corpora. We see that our collected MedWiki corpus leads to better QA performance by 0.9%-1.2% absolute. This result indicates that the MedWiki corpus can safely be used as a replacement of the MedQA corpus. The MedWiki yields USMLE accuracy that is superior to using the MedQA corpus (Table 11), and yields good results on the MedMCQA (Table 4) despite consisting in only of a fraction of the English Wikipedia.

Question	a 5 year old girl is brought to the emergency department by her mother because of multiple episodes of nausea and vomiting that last about 2 hours. during this period she has had 6-8 episodes of bilious vomiting and abdominal pain. the vomiting was preceded by fatigue. the girl feels well between these episodes. she has missed several days of school and has been hospitalized 2 times during the past 6 months for dehydration due to similar episodes of vomiting and nausea. the patient has lived with her mother since her parents divorced 8 months ago. her immunizations are up to date. she is at the 60th percentile for height and 30th percentile for weight. she appears emaciated. her temperature is 36.8 c. 98.8 f. pulse is 99 min and blood pressure is 82/52 mm hg. examination shows dry mucous membranes. the lungs are clear to auscultation. abdominal examination shows a soft abdomen with mild diffuse tenderness with no guarding or rebound. the remainder of the physical examination shows no abnormalities. which of the following is the most likely diagnosis?
Options	A: cyclic vomiting syndrome , B: gastroenteritis, C: hypertrophic pyloric stenosis, D: gastroesophageal reflux disease
Document from MedQA	headache, and sweating patient presentation : be is a 45 - year - old woman who presents with concerns about sudden (paroxysmal), intense, brief episodes of headache, sweating (diaphoresis), and a racing heart (palpitations). focused history : be reports that the attacks started 3 weeks ago, they last from 2 to 10 minutes, during which time she feels quite anxious. during the attacks, it feels as though her heart is skipping beats (arrhythmia). at first, she thought the attacks were related to recent stress at work and maybe even menopause. the last time it happened, she was in a pharmacy and had her blood pressure taken. she was told it was 165 / 110 mm hg. be notes that she has lost weight (~8 lbs) in this period even though her appetite has been good. pertinent findings : the physical examination was remarkable for be 's thin, pale
Document from MedWiki	panayiotopoulos syndrome . pial, or calcareous sulci. follow - up meg demonstrated shifting localization or disappearance of meg spikes. illustrative cases in a typical presentation of panayiotopoulos syndrome, the child looks pale, vomits, and is fully conscious, able to speak, and understand but complains of " feeling sick. " two thirds of the seizures start in sleep ; the child may wake up with similar complaints while still conscious or else may be found vomiting, conscious, confused, or unresponsive. case 1. a girl had 2 seizures in sleep at 6 years of age. in the first fit she was found vomiting vigorously, eyes turned to one side, pale, and unresponsive. her condition remained unchanged for 3 hours before she developed generalized tonic - clonic convulsions. she gradually improved, and by the next morning was normal. the second seizure occurred 4 months later. she awoke and told her mother that she wanted to vomit,

Table 12: An example of the retrieved documents from the MedQA and MedWiki corpus respectively. Correct answers and document titles are highlighted when available.

Question	a 40 year old woman presents with difficulty falling asleep diminished appetite and tiredness for the past 6 weeks. she says that despite going to bed early at night she is unable to fall asleep. she denies feeling anxious or having disturbing thoughts while in bed. even when she manages to fall asleep she wakes up early in the morning and is unable to fall back asleep. she says she has grown increasingly irritable and feels increasingly hopeless and her concentration and interest at work have diminished. the patient denies thoughts of suicide or death. because of her diminished appetite she has lost 4 kg. 8.8 lb in the last few weeks and has started drinking a glass of wine every night instead of eating dinner. she has no significant past medical history and is not on any medications. which of the following is the best course of treatment in this patient?
Options	A: diazepam , B: paroxetine, C: zolpidem, D: trazodone
Document from MedQA	headache, and sweating patient presentation : be is a 45 - year - old woman who presents with concerns about sudden (paroxysmal), intense, brief episodes of headache, sweating (diaphoresis), and a racing heart (palpitations). focused history : be reports that the attacks started 3 weeks ago, they last from 2 to 10 minutes, during which time she feels quite anxious. during the attacks, it feels as though her heart is skipping beats (arrhythmia). at first, she thought the attacks were related to recent stress at work and maybe even menopause. the last time it happened, she was in a pharmacy and had her blood pressure taken. she was told it was 165 / 110 mm hg. be notes that she has lost weight (~8 lbs) in this period even though her appetite has been good. pertinent findings : the physical examination was remarkable for be 's thin, pale
Document from MedWiki	hillary clinton's tenure as secretary of state . hillary to the middle east to talk about how these countries can transition to new leaders — though, i've got to be honest, she's gotten a little passionate about the subject. these past few weeks it's been tough falling asleep with hillary out there on pennsylvania avenue shouting, throwing rocks at the window. in any case, obama's reference to clinton travelling a lot was true enough ; by now she had logged in her boeing 757, more than any other secretary of state for a comparable period of time, and had visited 79 countries while in the office. time magazine wrote that "clinton's endurance is legendary" and that she would still be going at the end of long work days even as her staff members were glazing out. the key was her ability to fall asleep on demand, at any time and place, for power naps. clinton also saw the potential political changes in the mideast as an opportunity for an even more fundamental change

Table 13: An example of the two different retrieved documents from the MedQA and MedWiki corpus. Correct answers and document titles are highlighted when available.

Question	a 37 year old female with a history of type ii diabetes mellitus presents to the emergency department complaining of blood in her urine left sided flank pain nausea and fever. she also states that she has pain with urination. vital signs include temperature is 102 deg f. 39.4 deg c blood pressure is 114/82 mmhg pulse is 96 min respirations are 18 and oxygen saturation of 97 on room air. on physical examination the patient appears uncomfortable and has tenderness on the left flank and left costovertebral angle. which of the following is the next best step in management?
Options	A: obtain an abdominal ct scan , B: obtain a urine analysis and urine culture , C: begin intravenous treatment with ceftazidime, D: no treatment is necessary
Document from MedQA	rim, & quinolones camille e. beauduy, pharmd, & lisa g. winston, md * a 59 - year - old woman presents to an urgent care clinic with a 4 - day history of frequent and painful urination. she has had fevers, chills, and flank pain for the past 2 days. her physician advised her to come immediately to the clinic for evaluation. in the clinic she is febrile (38.5 °c [101.3 °f]) but otherwise stable and states she is not experiencing any nausea or vomiting. her urine dipstick test is positive for leukocyte esterase. urinalysis and urine culture are ordered. her past medical history is significant for three urinary tract infections in the past year. each episode was uncomplicated, treated with trimethoprim - sulfamethoxazole, and promptly resolved. she also has osteoporosis
Document from MedWiki	hydronephrosis . hydronephrosis describes dilation of the renal pelvis and calyces as a result of obstruction to urine flow. signs and symptoms the signs and symptoms of hydronephrosis depend upon whether the obstruction is acute or chronic, partial or complete, unilateral or bilateral. hydronephrosis that occurs acutely with sudden onset (as caused by a kidney stone) can cause intense pain in the flank area (between the hips and ribs). historically, this type of pain has been described as "diall's crisis". conversely, hydronephrosis that develops gradually will generally cause either a dull discomfort or no pain. nausea and vomiting may also occur. an obstruction that occurs at the urethra or bladder outlet can cause pain and pressure resulting from distension of the bladder. blocking the flow of urine will commonly result in urinary tract infections which can lead to the development of stones, fever, and blood or pus in the urine

Table 14: An example of the two different retrieved documents from the MedQA and MedWiki corpus. Correct answers and document titles are highlighted when available.